İSTANBUL TECHNICAL UNIVERSITY ★ ENERGY INSTITUTE

OPTIMIZATION OF TROMBE WALL PERFORMANCE USING COMPUTATIONAL FLUID DYNAMICS AND BUILDING ENERGY SIMULATION

M.Sc. Thesis by
Güven ÖĞÜŞ

Department of Energy Science and Technology

Energy Science and Technology Programme

JUNE 2013

İSTANBUL TECHNICAL UNIVERSITY ★ ENERGY INSTITUTE

OPTIMIZATION OF TROMBE WALL PERFORMANCE USING COMPUTATIONAL FLUID DYNAMICS AND BUILDING ENERGY SIMULATION

M.Sc. Thesis by
Güven ÖĞÜŞ
301101021

Department of Energy Science and Technology

Energy Science and Technology Programme

Thesis Supervisor: Assist. Prof. Dr. Murat ÇAKAN(İTÜ)

JUNE 2013

İSTANBUL TEKNİK ÜNİVERSİTESİ ★ ENERJİ ENSTİTÜSÜ

HESAPLAMALI AKIŞKANLAR DİNAMİĞİ VE BİNA ENERJİ SİMÜLASYONU KULLANILARAK TROMB DUVARLARDA PERFORMANS OPTİMİZASYONU

YÜKSEK LİSANS TEZİ

Güven ÖĞÜŞ
301101021

Enerji Bilim ve Teknoloji Anabilim Dalı

Enerji Bilim ve Teknoloji Programı

Tez Danışmanı : Yrd. Doç. Dr. Murat ÇAKAN(İTÜ)

HAZİRAN 2013

İTÜ, Enerji Enstitüsü'nün 301101021 numaralı Yüksek Lisans Öğrencisi Güven ÖĞÜŞ, ilgili yönetmeliklerin belirlediği gerekli tüm şartları yerine getirdikten sonra hazırladığı "Optimization Of Trombe Wall Performance Using Computational Fluid Dynamics And Building Energy Simulation" başlıklı tezini aşağıda imzaları olan jüri önünde başarı ile sunmuştur.

Tez Danışmanı : Yrd. Doç. Dr. Murat Çakan .....

İstanbul Teknik Üniversitesi

Jüri Üyeleri : Doç. Dr. Hatice Sözer .....

İstanbul Teknik Üniversitesi

Yrd. Doç. Dr. Levent Kavurmacıoğlu .....

İstanbul Teknik Üniversitesi

Teslim Tarihi : 02 Mayıs 2013

Savunma Tarihi : 03 Haziran 2013

FOREWORD

I would like to express my gratitudes for my advisor Dr. Murat Çakan for his patience and helpful comments during this study. Also I want to thank Energy Institue for supporting this thesis with computational facilities

TABLE OF CONTENTS

Page

ABBREVIATIONS

CFD	**:** Computational Fluid Dynamics
BES	**:** Building Energy Simulation
RMS	**:** Root Mean Square
Re	**:** Reynolds Number
Nu	**:** Nusselt Number

LIST OF TABLES

Page

LIST OF FIGURES

Page

OPTIMIZATION OF TROMBE WALL PERFORMANCE USING COMPUTATIONAL FLUID DYNAMICS AND BUILDING ENERGY SIMULATION

SUMMARY

For reducing the fossil fuel demands, using renewable energy sources as much as possible in buildings is a widely studied topic. All kinds of buildings are important energy consumers. Most of this energy is consumed for heating purposes. The direct application of heating availability of solar energy on buildings is a very efficient way to decrease this demand. For the winter season when the heating demand is maximum benefiting from sun as much as possible is important. This can achieved by only introducing different building element designs. Thermal or Trombe walls are used to benefit from sun as much as possible. A Trombe wall is usually a concrete or brick wall that is behind a glazing. The principle is to capture the radiation heat between glazing and the wall behind it. This causes the wall to heat. It is a thermal storage for nights and a ventilation tool for day conditions. In this study, the performance of this type of wall is optimized using two main tools; Building Energy Simulation and Computational fluid dynamics. A temperature measurement is made on an actual space with a Trombe wall. Building energy simulation tools are very efficient for determining a time ranged analysis of building energy demand, heating conditions, space temperatures. This tool is also efficient for determining the solar heat gains. The solar radiation is estimated with powerful solar models for diffuse and direct radiation. For comparison, measurements on an actual house model with a Trombe wall installed located in ITU Mechanical Engineering campus. Though both experiment and building energy simulation are good tools for optimization estimation, the complex flow inside the space is a problem to be solved considering several parameters such as turbulence, natural convection and buoyancy. With the boundary conditions calculated from these tools a CFD study has been made in a space model. The aim of the optimization is to compare different dimensions of vents

and space between glazing and the storage wall. As it affects the storage properties of the wall, storage wall material is also varied to see the change of storage capacity of the wall. The CFD study is made both in a two dimensional and a three dimensional domain. Two dimensional calculations are for optimizing the geometrical parameters in a specific time range. Using building energy simulation and computational fluid dynamics together, a coupled solution of both is desired. Also with three dimensional CFD analysis, the flow inside the space and the buoyancy effects caused by solar heating. Also the flow pattern inside the heated space is observed using a 3D computational fluid dynamics analysis.

HESAPLAMALI AKIŞKANLAR DİNAMİĞİ VE BİNA ENERJİ SİMÜLASYONU KULLANILARAK TROMB DUVARLARDA PERFORMANS OPTİMİZASYONU

ÖZET

Fosil yakıt taleplerini azaltmak için, binalarda yenilenebilir enerji kaynaklarının mümkün olduğunca çok kullanılması çokça çalışılan bir konudur. Her çeşit bina önemli enerji harcayıcılarıdır. Binalarda enerjinin büyük kısmı ısıtma amaçlarıyla kullanılmaktadır. Güneş enerjisinin direkt ısıtma amacıyla kullanılması bu harcamayı önemli biçimde azaltabilmektedir. Isıtma talebinin en yüksek olduğu kış aylarında güneşten en verimli şekilde faydalanabilmek önemlidir. Türkiye güneş açısından özellikle şanslı olmakla beraber, bu kaynaktan henüz yeterince verimli faydalanamamaktadır. Güneş enerjisinin elektrik ve buhara çevrilerek kullanılması yaygınlaşmaya başladıysa da, konutlar, ticari binalar gibi yapılarda ısı amaçlı kullanımında farklı yaklaşımlar tartışılabilinir. Bu amaç için özel tasarlanmış yapı elemanlarının eklenmesi verimli faydalanma için yeterli olabilmektedir. Termal, diğer adıyla Tromb duvarlar, bu amaç için tasarlanan, güneşin ışınım enerjisini en yüksek seviyede kullanmak üzerine kurulu sistemlerdir. Tromb duvarlar, bir cam pencere cephenin arkasındaki genelde beton ya da tuğladan yapılan duvarlardır. Cam güneş ışınımını geçirir, ve arkasında kalan termal duvar olarak tabir edilen yüzeyi ısıtır. Bu ısı, camın sağladığı bir tür sera etkisi yardımıyla uzun süre kaybolmamaktadır. İletim yoluyla, duvarın arkasında kalan ısıtılan bölgeye geçer. Aynı zamanda, duvarla cam arasındaki boşluk ve ısıtılan mekan duvar üzerine açılan üst tarafta ve alt tarafta olan menfezlerle bağlıdır. Duvarın ısınmasıyla yükselen hava üstteki menfezlerden mekana girerken, alttaki menfezlerden de boşluğa mekandaki hava girmektedir. Bu etkiyle beraber mekan, doğal taşınım yoluyla da ısıtılmış olur. Aynı zamanda gündüz vakti duvar dış mekana göre sıcak kalmaktadır. Bütün bunların sonucu duvar, geceler için ısı deposu ve gün koşulları için ısıtma ve havalandırma sistemi olarak kullanılır. Bu cephe bileşeninin performansı geometrik değişkenler ve kullanılan malzeme ile doğrudan ilişkilidir. Bu çalışmada, bu tip bir

duvarın performans optimizasyonu iki temel araç kullanılarak yapılmıştır; Bina enerji simülasyonu ve hesaplamalı akışkanlar dinamiği (HAD). Aynı zamanda gerçek bir Tromb duvarlı mekan içinde sıcaklık ölçümleri yapılmıştır. Bina enerji simülasyonu zamana yayılmış, mevsimsel etkileri de göz önüne alacak şekilde ısıtma soğutma yüklerinin belirlenmesinde, güneş ısıtmasının etkisini de göz önüne alarak hesaplanmasında oldukça etkili bir araçtır. Bu simülasyon yönteminde kullanılan güneş ışınım modelleri oldukça güçlüdür. Bu çalışmada kış ve bahar şartlarında Tromb duvarı modellemek için, bir cam kaplama arkasında kalan bir duvarın güneş ışınımı ısı kazanımı hesaplanmıştır. Duvarın kaplama malzemesinin bu ısı kazancına ne kadar etki ettiği farklı emicilik değerleri kullanılarak görülmüştür. Bina enerji simülasyonu aynı zamanda iç mekan sıcaklığını ve ısı kazançlarını geometrik değişkenler için karşılaştırmak için de kullanılabilir. Ancak özel koşulların olduğu Tromb duvar sisteminde özel akış koşulları vardır. Kaldırma kuvveti ile hava hareketi ve doğal taşınılma ısı transferi etkileri bina enerji simülasyonunda tam olarak modellenememektedir. Bu durumun daha iyi optimizasyonu için güneş ışınımı ısı kazancı sınır koşul olarak kullanılarak hesaplamalı akışkanlar dinamiği simülasyonları yapılmıştır. Bu analiz hem iki boyutlu hem üç boyutlu olarak yapılmıştır. Analizin doğrulanması için, İTÜ Gümüşsuyu kampüsünde bulunan gerçek bir Tromb duvarlı mekan içinde 5 günlük sıcaklık değerleri ölçülmüştür. Bu değerler HAD simülasyonunun doğruluğunu ve sapmasını bulmak için kullanılmıştır. Ayrıca gerçek ısıtma etkisinin de gözlemlenmesi açısından ölçümler yorumlanmıştır. İki boyutlu HAD analizi, bina enerji simülasyonunda hesaplanan güneş ısı kazancı değerleri kullanılarak zamana bağlı şekilde gerçekleştirilmiştir. Bu analizler, farklı menfez boyutları ve farklı cam ile duvar arasında kalan boşluk boyutları için tekrar edilmiş ve en verimli ısıtmayı sağlayan geometrik kurulum tespit edilmeye çalışılmıştır. Farklı durumlar için farklı optimum geometriler olduğu görülmüştür. Isıtma aynı zamanda, duvarın yapıldığı malzemeden de etkilenmektedir. Duvar malzemesi olarak alüminyum, ahşap ve beton modellerde analizler yapılmıştır. Farklı durumlarda optimum ısıtmayı sağlayan malzemeler tespit edilip yorumlanmıştır. Zamana bağlı iki boyutlu analizlerden sonra, mekan içerisindeki karmaşık akış

halini gözlemlemek için üç boyutlu analizler yapılmıştır. Uygun sayısal ağ ve geometrik modeller hazırlanmış, gerekli fiziksel modellerin incelenmesi yapılmıştır. Bu analizlerin sonucunda, mekan ve Tromb duvar önündeki boşluk içindeki hava hareketleri gözlemlenmiştir. Türbülans, ani hız kayıpları gibi ısı transferini etkileyecek noktalar tespit edilmiştir. Bu çalışma, bina enerji performansı belirlenmesinde yaygın kullanılan hesaplamalı akışkanlar dinamiği ve bina enerji simülasyonu araçlarının beraber kullanımı ile pratik kullanıma uygun bir yöntem uygulamasıdır.

1. INTRODUCTION

1.1 Energy, Buildings and Sun

The energy consumption of the households in Europe, according to European commission statistics, is 26.7% of the whole energy consumption in Europe, seen in Figure 1.1 [1]. The achievement goal for energy consumption for 2020 is %20 reduction. It is obvious that to achieve this goal, energy consumption in households should be reduced.

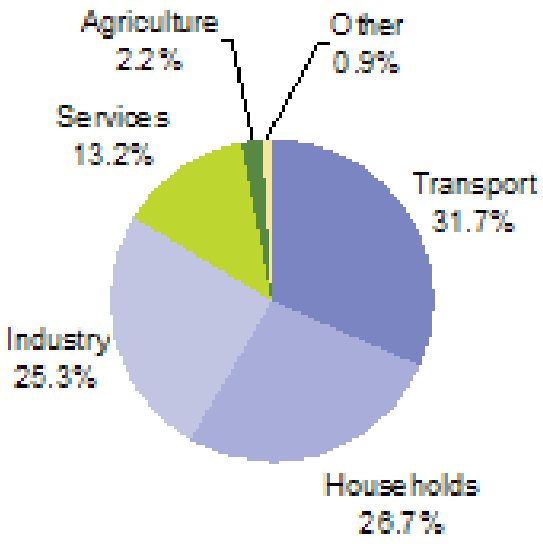

Figure 1.1 : Distribution of energy consumption to sectors in europe.

One more goal for 2020 to achieve for Europe is to increase the usage of renewable energy sources in all areas. Figure 1.2 shows the type of primary energy source usages by sector. As seen, households use natural gas in a big ratio. Most of this consumption is for heating purposes. The usage of renewable energy, mostly sun, could be possible.

Usage of sun more and more would be beneficial to reduce fossil fuel uses and reduce carbon emissions. The passive house or solar house concept is based on using the solar irradiation for heating.

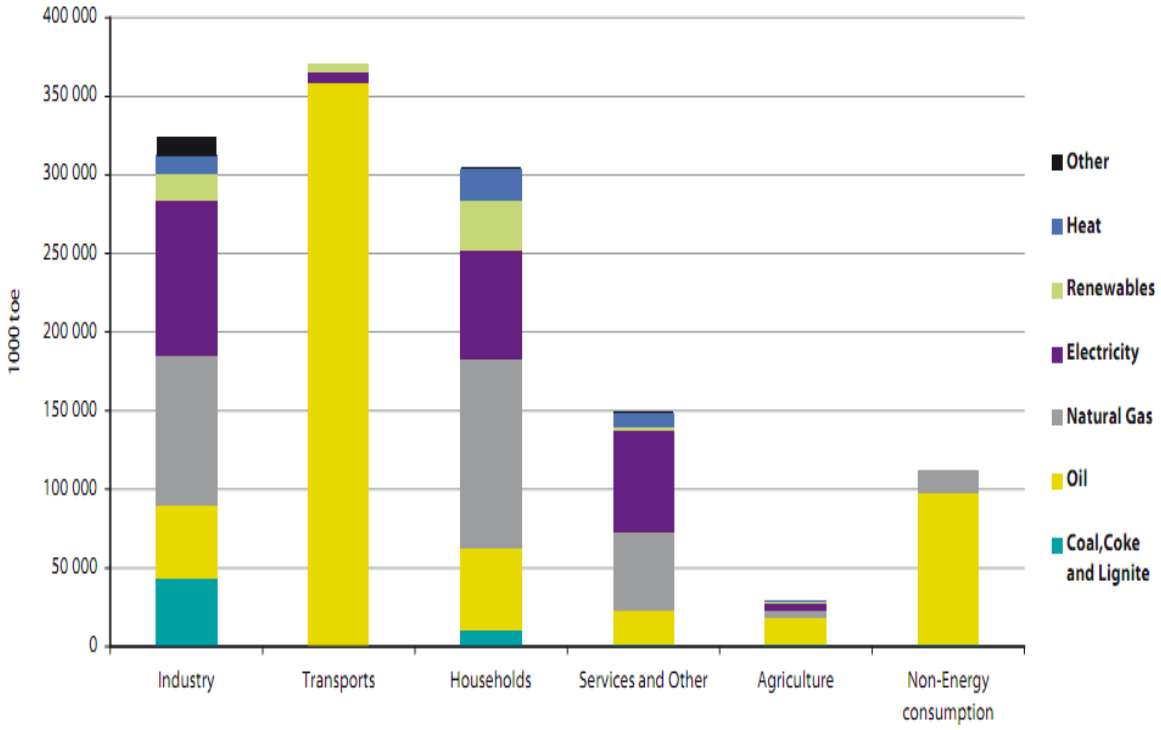

Figure 1.2 : Primary energy sources usage distribution to the sectors.

For passive house designs, getting maximum heating energy from solar radiation energy for heating in winter season is essential. Figure 1.3 shows the solar irradiation map for Europe. Especially Mediterranean countries have a very high potential of solar irradiation.

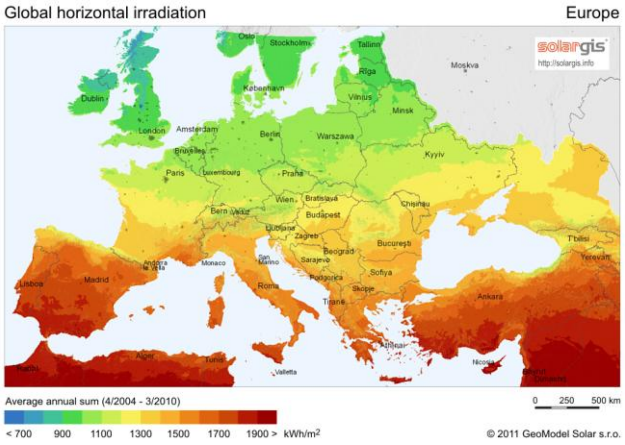

Figure 1.3 : Solar map of Europe [2].

Turkish State Meteorological Service (Meteoroloji Genel müdürlüğü) statistics (Table 1.1) states that average daily sunshine hours for the densest settled regions Ankara and İstanbul are about 2-5 hours. That will be a very good potential for winter heating energy demand savings.

Table 1.1 : Ankara – İstanbul annual sunshine statistics [3].

		Jan.	Feb.	March	April	May	June	July	Agust	Sept.	Oct.	Nov.	Dec.
Ankara	Avarage Daily Sunshine Time (Hours)	2.4	3.5	5.3	6.3	8.4	10.3	11.3	10.5	9.2	6.4	4.2	2.2
İstanbul	Avarage Daily Sunshine Time (Hours)	2.2	3.1	4.3	6	8.1	9.5	10.3	9.3	7.6	5.1	3.3	2.2

1.2 Passive House

Passive house is defined as -

"Passive House is both a building energy performance standard and a set of design and construction principles used to achieve that standard. The Passive House standard is the most stringent building energy standard in the world: buildings that meet the standard use 80 percent less energy than conventional equivalent buildings, and provide superior air quality and comfort."

- by the United States Passive House Alliance [4].

There are several methods and several approaches to achieve the 80% energy saving goal for passive house designs.

The focus is on the mechanical heating/cooling systems, ventilation systems mostly. Solar houses are an efficient way to use the solar heat efficiently. Very widely used elements of solar houses are Trombe walls. A trombe wall is a south facing, usually concrete or brick wall that is placed behind an insulated glazing. The sun facing side of the wall is generally coated with a black selective surface paint in a way that its absorptive properties for solar energy are increased. The main principle is to store the thermal energy inside the walls' thermal mass which depends on its thickness and material. Also, air in the gap between the wall and the glazing is a good ventilation thermal storage. It can be used to ventilate the space with heated air to help the

mechanical heating or for standalone heating purposes. At nights, the trombe wall acts as a thermal storage, and heats the space with the stored energy in it in the daytime.

An example to contribution of Trombe walls to energy saving is a study by Chel, Nayak and Kaushik in 2008. Study shows that a storage building of 25 m2 in India is calculated to have 3312 kWh/year energy saving just by introducing a Trombe wall. [5]

1.3 Research Objectives

The main purpose of this thesis is to find the affects of different parameters such as geometry and material properties to a solar wall passive house. A measurement configuration, usage of building energy simulation and computational fluid dynamics on passive houses is assessed.

To organize a summary for analyzing usage of several tools on a solar wall passive house is also a target. These would be the tools for a possible improvement of solar wall performance research for future.

Together with an actual optimization case, method suggestions on analysis are aimed.

1.4 Structure of the Study

Purpose of this study is to optimize several parameters that are expected to affect the performance of solar wall heating system. Tools such as actual measurements, building energy simulation and computational fluid dynamics are used for the purpose.

Firstly, in Chapter II, a literature review about passive house design, parameters and past studies is presented. Then the tools that are used in this thesis are introduced.

Secondly, the studied solar wall case is introduced and the actual measurements on the system are presented on Chapter III.

After introducing the case, the Building Energy Simulation fundamentals are reviewed and a study about the solar wall heat gain dependence on the solar wall thermal absorption ability is conducted and presented in Chapter IV. Also the

boundary conditions for the next study, the CFD, are calculated and presented in this chapter.

Chapter 5 assesses the computational fluid dynamics and Ansys CFX software fundamentals in the first part. Then, a time dependent 2D analysis and a steady state 3D study are presented. The comparison of variation of several parameters is discussed in this chapter with CFD simulations. Also, the general look of the inside flow and heat transfer with respect to different configurations is presented both in 2D and 3D cases.

The structure of the study requires all chapters to be connected to each other. Several tools are used for the study and they are all connected in several way. They all have different outputs and inputs that sometimes use another tool's output. Figure 1.4 summarizes the connection between the study parts and tool inputs, outputs. This figure and structure will be revisited at some points to explain more detail about steps.

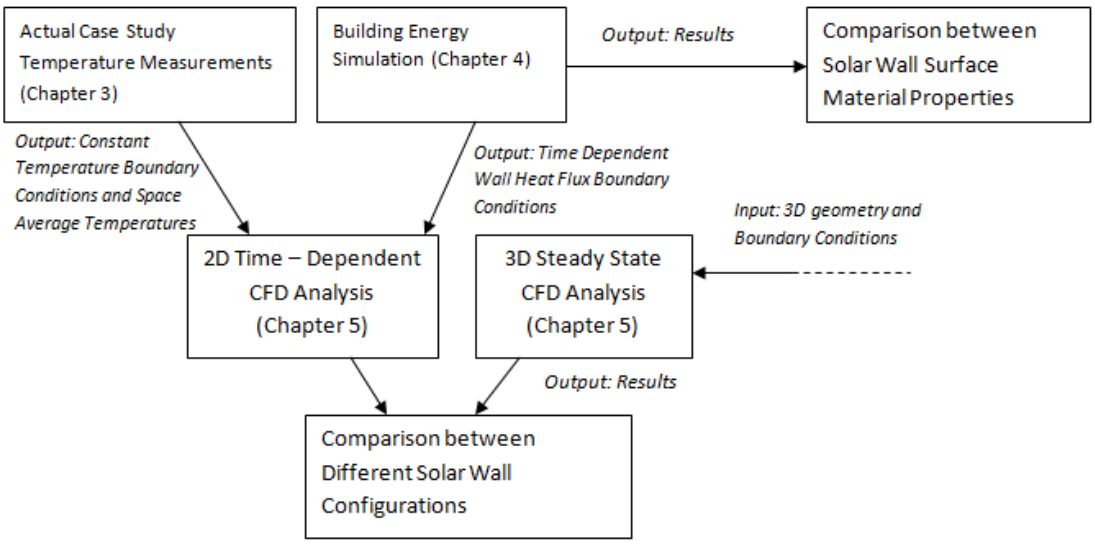

Figure 1.4 : The Connection between Chapters and Study Steps.

2. LITERATURE REVIEW

2.1 Solar House and Trombe Walls (Solar Walls)

Solar house concept mainly is related with usage of sun efficiently. The most widely used method is solar walls, called, Trombe walls or thermal storage walls.

Thermal storage wall design manual by Alex Wilson classifies the Trombe walls mainly into two categories. Vented and unvented. Figure 2.1 shows the schematic of these two main configurations.

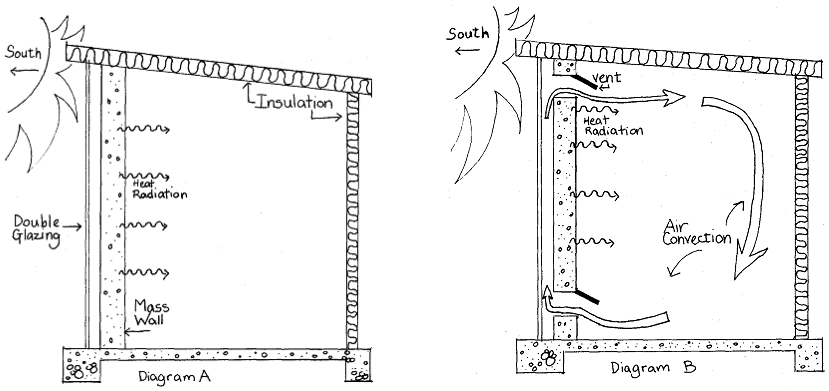

(a) (b)

Figure 2.1 : Main trombe wall configurations (a) unvented (b) vented case [6].

The main principle is to use heat gains from the sun as much as possible. In the unvented case, all heat gain is transmitted to the heated area by conduction. The vented case also uses the temperature of the south wall on the solar wall to induce natural convection, thus, air movement. Conduction and convection heat transfer mechanisms both occur in this case.The solar wall affects as a thermal mass, so heat storage. The stored heat inside the solar wall helps heating also at nights.

The Trombe wall can be classified as vented and unvented. The vented Trombe walls have vents on upper and lower side of the Trombe so that to let the air to circulate in the occupied space. In unvented Trombe wall systems, only the thermal storage property of the wall is in use. Vented Trombe walls use ventilation as a heating

mechanism. Though, heated air ventilation is preferred in Europe, an EnergyPlus code improver Ellis, states that in US unvented Trombe walls are more popular because it is a challenging problem to normalize the air flow rates in vented systems. [7]

There are several designs of vented solar wall in order to optimize the performance and ventilation affects. Some of these designs use outside air to induce the ventilation in order to acquire fresh air to the ventilated space. Some designs focus on the internal air circulation, aiming for increasing the heat gain. Figure 2.2 shows some of these designs.

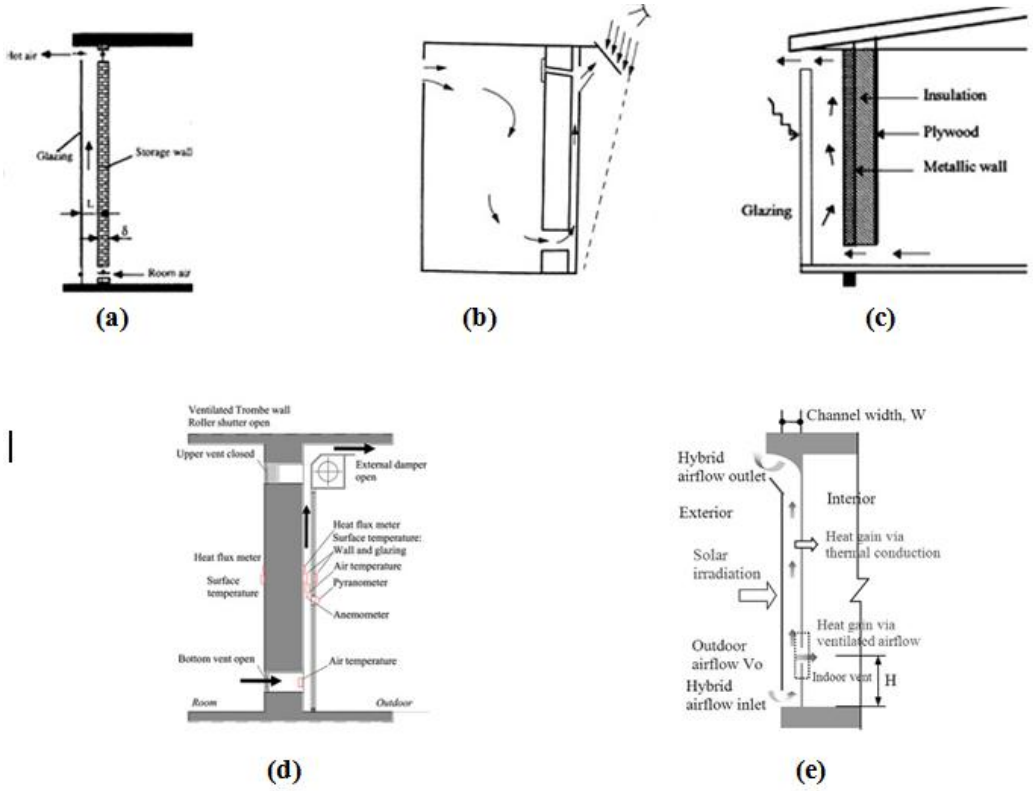

Figure 2.2 : Various Trombe Wall Designs **(a)** Trombe wall for summer cooling (Gan, 1998, [8]) (**b)** Trombe wall with cross ventilation and overhangs (Ghrab - Morcos, 1993, [9]);**(c)** natural ventilation by metallic solar wall (Hirunlabh, 1999 [10]); **(d)** ventilated solar wall with roller shutter and external damper (Stazi, 2012,[11]) **(e)** both inside and outside air ventilate solar wall (Lai, 2011, [12]).

The configuration (a) in Figure 2.2, by Gan, 1998, suggests a design that takes the hot air from the main space in summer condition, thus ventilates the space. The air movement is like a stack effect in the Trombe space.

The configuration (b) by Ghrab-Morcos, 1993, offers a shading device for usage in summer conditions. In very hot climates like Tunisia, though winter heating is needed, overheating is a big problem for summer conditions with solar walls. This design is claimed to eliminate this overheating problem in summer conditions.

The design (c) by (Hirunlabh, 1999 [10]) again focuses on summer conditions. This time, using a metal solar wall, with the same principle as (b) but without shading. Numerical study and experiments show the most efficient way to remove heat by a solar wall is to use a metal wall.

The configuration (d) by (Stazi, 2012, [11]) uses a manual control shutter for the inside vents, and a wall shader that is controllable to maintain heat inside at nights and to block the sun in the summer times.

The design (e) by (Lai, 2011, [12]) is a design that has vents both to inside space and outdoor air. The advantage of this design is together with both convection and conduction heat gains; it also provides fresh air inside the Trombe space.

Although there is countless number of solar wall designs, these examples are the most widely used ones, to explain the basic principles.

Also several designs are patented and being used as commercial products. The SolarWall® Company commercially produces and applies several patented solar wall systems on buildings, with claim of energy efficiency [13]

Also some designs offer different usages of Trombe Walls. This uses the heat gain not only for heating but also for generating electricity. Studies by (Lai, 2011, [12]) and Koyunbaba, B.K. [14], are examples for these studies. The main principle is to use the heat gain not only for heating the space but also for generating electricity.

The problem for the vented trombe wall is the control of the ventilation flow rates. There are several studies regarding this problem. For example a study by Liu, 2013, [15] offers an opening and closing mode controlled vent on the thermal wall. With further studies in this area, it is sure to have a very effective control strategy for the air flow rates in close future. A review of opportunities in this research area studied by Saadatian O. 2012 [16], foresees that this ventilation rate control topic will be a very good interest of study in the close future.

This study investigates the classical vented Trombe wall systems.

Figure 2.3 shows the schematic of a classical Trombe wall which will be assessed in this thesis.

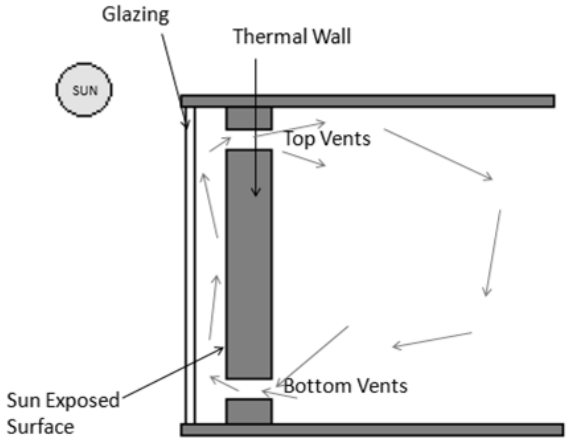

Figure 2.3 : The vented (classical) trombe wall configuration.

The vented Trombe wall supports the mechanical heating with the extra heated air supply to the space.

The performance of a vented Trombe wall are governed by, radiation heat transfer to the sun exposed surface, conduction in the thermal wall, heat storage capacity in the thermal wall and free convection.

The most complicated calculation of this heat transfer schema is the free convection. The air velocity, air flow rate, 3 dimensional size of the gap all affects the performance. The free convection flow in the gap includes turbulent flow. There are some analytical and finite difference methods for calculating the free convection parameters in the gap. But a numerical cell grid based analysis would give the best result.

The air movement, induced by natural convection in the gap, flows through the top vents on the Trombe wall and circulates in the occupied space. Then as the air flowing to the space cools down, its density increase and flows to the bottom vents through the gap again. Basic physics behind all this air and energy movement is natural convection.

As the natural convection is the main mechanism, for the rate of energy and air flow, gap thickness, wall temperatures, Trombe wall thermal storage capacity is the main parameters.

Duffie and Beckman, 2006 [17] states that, for turbulent flows inside a gap Nusselt number in a ventilated trombe wall space can be defined as;

$$Nu = 0.0158Re^{0.8} \quad \textbf{(2.1)}$$

For the laminar zone, the same calculation can be made with,

$$\mathrm{Nu} = \frac{0.0606\left(\frac{\mathrm{RePrD_h}}{\mathrm{L}}\right)^{1.2}}{1+0.0909\left(\frac{\mathrm{RePrD_h}}{\mathrm{L}}\right)^{0.7}\mathrm{Pr}^{0.17}} \quad \textbf{(2.2)}$$

Where

$$\mathrm{Nu} = \mathrm{h_f}.\mathrm{L} / \mathrm{k_f}\,, \quad \textbf{(2.3)}$$

$$\mathrm{Re} = {}^{\mathrm{V}.\mathrm{D_h}}/_{\upsilon}\,, \quad \textbf{(2.4)}$$

and

$$\mathrm{Pr} = {}^{C_p\,\mu}/_{k_f} \quad \textbf{(2.5)}$$

k_f is the thermal conductivity in W/m.K; h_f is the convection heat transfer coefficient (W/m^{2}K) and L is the characteristic length in meters. V is the velocity while D_h is the hydraulic diameter.

These equations are for calculating the convection heat transfer coefficient in the air gap.

There are several other parameters to calculate for a trombe wall and there are several offered methods from authors. The most widely accepted one of these methods is an explanation in the standard ISO13790 Energy performance of buildings — Calculation of energy use for space E.4 section Trombe wall calculations. [18] According to this standard in winter conditions and summer conditions following rules apply;

"*– the air flow is stopped automatically when the air layer is colder than the heated space and during summer,*

– the air flow rate is set mechanically at a constant value, when the air layer is warmer than the heated space."[18]

These rules obviously propose a mechanical control system on vents. This thesis assesses the heating condition of the Trombe walls.

According to the standard, two aspects play main role in the calculations; heat transfer coefficients and solar heat gains from by the thermal wall.

Heat transfer coefficient can be calculated as

$$h = h_o + \Delta h \quad \textbf{(2.6)}$$

Where,

h_0 is the heat transfer coefficient of the non-ventilated wall;

Δh is the additional heat transfer coefficient from ventilating effects

$$\Delta h = \rho_a c_a q_{ve,sw} \left(\frac{U_e}{U_i}\right)^2 \delta K_{sw} \quad \textbf{(2.7)}$$

Where, $\rho_a c_a$ is the heat capacity of air per volume;

δ here, is the ratio accumulated internal-external temperature difference when the ventilation is on, to its value over the whole calculation step

$$U_i = \frac{1}{R_i + \frac{R_l}{2}} \quad \text{and} \quad U_e = \frac{1}{R_e + \frac{R_l}{2}} \quad \textbf{(2.8)}$$

R_i is the internal thermal resistance of the wall, between the air layer and the internal environment,

R_e is the external thermal resistance of the wall, between the air layer and the external environment,

R_l is thermal resistance of the air layer;

A new parameter is defined as;

γ_{al} , which is the heat gain to heat loss ratio of the air layer.

$$\gamma_{al} = \frac{Q_{Gain}}{Q_{loss}} \quad \textbf{(2.9)}$$

The solar gains and the losses must be known to calculate this parameter

This is used for calculation of δ as;

$$\delta = 0.3\gamma_{al} + 0.03(0.003^{\gamma_{al}}\text{-}1) \quad \textbf{(2.10)}$$

And K_{sw} is a factor defined by solar wall area and ventilation flow rate from the thermal zone to the space.

The method suggests using this calculated Δh and h_o values; it is possible to correlate the solar heat gains to the heat balance of the wall;

Defining ω as solar radiation ratio falling on the thermal element, this should be calculated with radiation correlations; the relation is;

$$\omega = 1 - \exp(-2{,}2\gamma_{al}) \quad \textbf{(2.11)}$$

Figure 2.4 shows the relation between these two parameters.

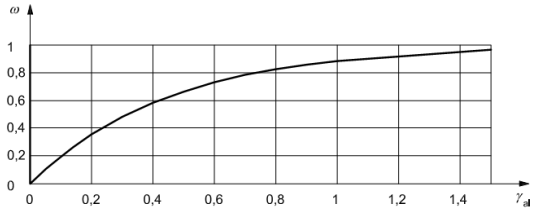

Figure 2.4 : Ratio ω of the total solar radiation falling on the element when the air layer is open to the total solar radiation during the calculation step, as a function of the heat-balance ratio of the air layer.

Though, these equations and relations are most widely accepted as it is presented in a standard ISP 13790, a study made by Ruiz-Pardo, Domíngues and Fernández at 2010, [18] shows that these equations do not perfectly match the real situation. The study uses a resistor model analogy to calculate the heat transfer coefficients and heat gains and they are compared with actual data.

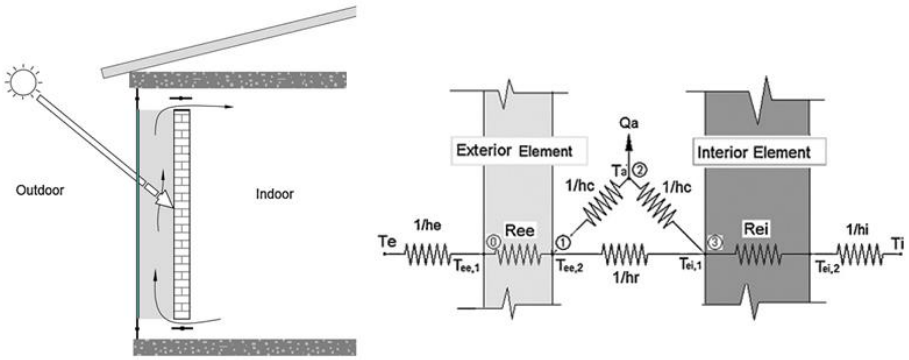

(a) **(b)**

Figure 2.5 : The wall resistor analogy **(a)** physical schematic **(b)** triangular wall resistor analogy.

There are several equation derivations like this that can be found in literature. These equations can be considered as case specific correlations. Using resistor model analogy, problem can be solved numerically for each problem individually as in Building Energy Simulations (BES) and a more accurate calculation can be made with computational fluid dynamics (CFD) and experimental methods. Also the complexity of these equations needs a computational tool for calculation.

A very good example for BES study on solar walls is made by Shen, 2007 [20] using TRNSYS energy modeling software. Also this paper names the internal air circulating solar wall as the classical Trombe wall, which this thesis focuses on.

A CFD study of a ventilated Trombe wall is made by Hami, K., 2012 [21]with a low resolution 2D grid. Also a combination of experimental study and 2D CFD analysis is made by Koyunbaba, 2011 [13]. This study shows the real situation and a well configured CFD simulation holds for results reasonably.

BES can also be used to optimize the Trombe wall geometry. "Optimum design of Trombe wall system in Mediterranean region" by Jaber and Ajib, 2011 [22] is a very good example of such studies. It demonstrates the solar wall optimization for a whole building for Mediterranean climate. Also a life cycle cost analysis which is essential for energy saving projects is made in this analysis. Figure 2.6 Shows the life cycle cost economical analysis from this study.

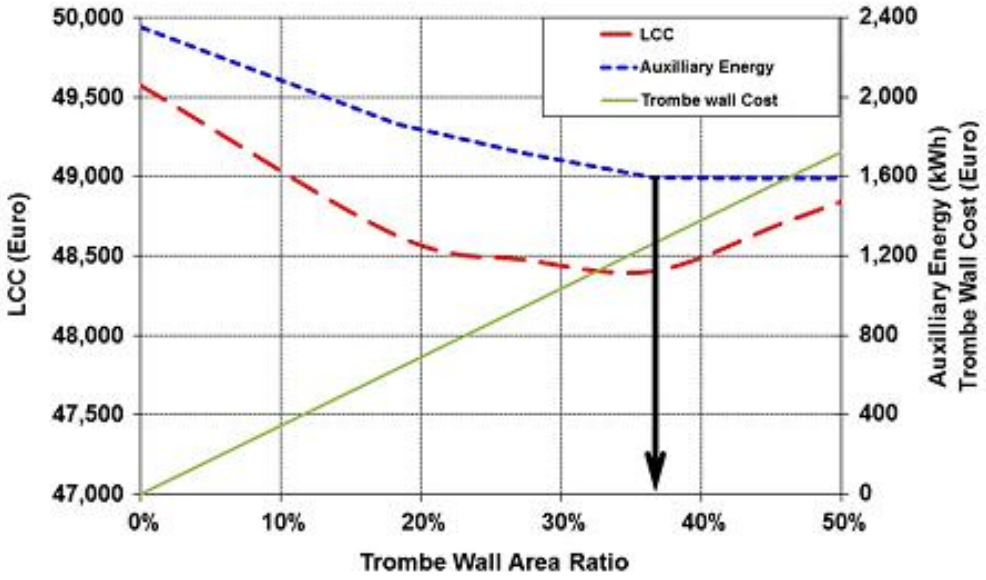

Figure 2.6 : Life cycle cost analysis vs. trombe wall area ratio.

This figure is obtained in the cited study by calculating the heating performance with respect to solar wall ratio to the whole building façade ratio. The LCC curve represents the total life cost of the system while auxiliary energy is the cost analysis of the energy used to heat the building. As seen from the figure, solar walls can be beneficial with special conditions. The optimum cost is calculated with this method. Study claims it is possible to save around 1200 Euro's annually using an optimized solar wall system, with respect to a configuration with no trombe wall configuration.

This thesis focuses on the flow and geometrical optimizations but no economical aspects for the solar wall installation. In commercial applications, life cycle cost analysis should be done in order to determine the savings.

There are also several experimental approaches to the solar houses. Previously mentioned study made by Shen (2007) [20] is an example of an experimental study on several ventilation strategies, in order to increase the thermal performance and optimize the ventilation rates of the solar wall using experimental methods.

Also previously mentioned study by Stazi (2012) [11] is a very detailed experimental study that compares different trombe wall configurations.

A discussion for the experimental methods on solar walls is made by Onbasioglu and Egrican in 2002 [23]. The discussion suggests an experimental procedure and the sensitivities of the experiments on solar walls. It states that the solar wall temperature is very sensitive to rapid changes in the solar irradiation data. This study uses the very same solar house located in İTÜ/Gümüşsuyu Campus.

There are also several studies using CFD for determining and optimization of the performance of solar walls.

Study by Uygur and Egrican done in 1995 [24] is a mathematical and numerical approach on a passive heated zone. The study includes an optimization for trombe spaces according to some geometrical variables. Also turbulence and approach to the general flow equations in the cavity is discussed in detail.

The conference paper by Hamza and Underwood presented in 2005 [25], assesses the thermal performance of a solar wall using both BES and CFD. This study uses a general approach to the double skin façades that may be generalized with special attention to solar walls.

Also, a study about visualization of the temperature and velocity distribution in a solar house with boundary condition reductions is made by Mezhrab and Rabhi in 2008. The study shows a good example of CFD study on the trombe wall with nondimensionalized geometric parameters.

There are several approaches in all these studies. This thesis is a study to optimize geometrical variables on a simple one zone heating with a solar wall. Also all tools, BES, CFD and experiment are used in this study.

3. ACTUAL CASE AND MEASUREMENTS

3.1 The Real Case, Experimental Method and Setup

The first stage of the study is to find out the actual temperature variations in a solar house. Later, the case comparison about geometry and material properties will be discussed on the house that the measurements are taken from. For the purpose, temperature measurements are made on the solar house that has been built in 1998, located in Istanbul Technical University, Gümüşsuyu/ İstanbul is used.

(a)

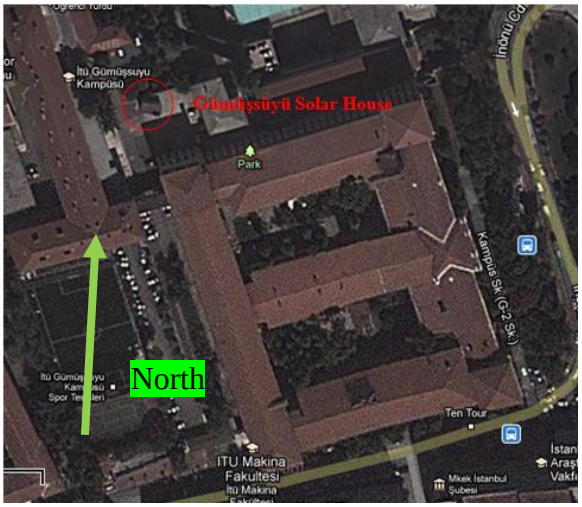

(b)

Figure 3.1 : The gümüşsuyu solar house **(a)** photo **(b)** location.

Several other studies have been conducted in this same solar house. Those studies will be referenced on some points of this study.

Figure 3.1 (a) shows an actual photograph of the studied solar house and (b) is a Google Earth image of the solar house location. As the solar house is located very near the center of İstanbul, using the meteorological data of İstanbul would be reasonable.

Figure 3.2 : The experiment setup.

The test cell is a box shaped space with 3.3x 3.3 x 3.0 m dimensions. It also has a Thermal wall which faces the ambient and sun through glazing. The thermal wall has 8 vents whose dimensions are 0.2x0.5 m. Four of them are placed at the bottom of the solar wall while four of them are on the top. The thermal wall thickness is 0.15 m. and the distance between glazing and the Trombe wall is 0.2 m. The material of all construction is accepted as concrete. Detailed dimensions of the space and a schematic can be seen on Figure 3.3.

The wall temperatures are collected with a KEITHLEY 2700 data acquisition system connected to 18 K-type thermocouples. The device has been connected to a computer to collect data over 6 days. Data has been collected in every 20 minutes from 18 channels. The thermocouples are attached to the inside walls to observe the temperature variations in the space. Also, a thermocouple has recorded the temperature of the midpoint of the room. The midpoint temperature is actually the targeted temperature and optimizations should be made in order to increase the space temperature on seasons that heating is demanded. The measurements are made through April 5-12 which have moderate weather conditions. All wall temperatures

and the Trombe space glazing temperature are measured, along with space average temperature. The experiment setup is seen on figure 3.2

As the idea behind this solar house is to heat the space with the heat gain of the solar (Trombe) wall, the measurements on the trombe space has also been made.

The data is collected from the solar wall outside surface which is exposed to sun and from the glazing as well as the main space walls. A schematic of the solar house and the placement of the thermocouples are seen on Figure 3.3.

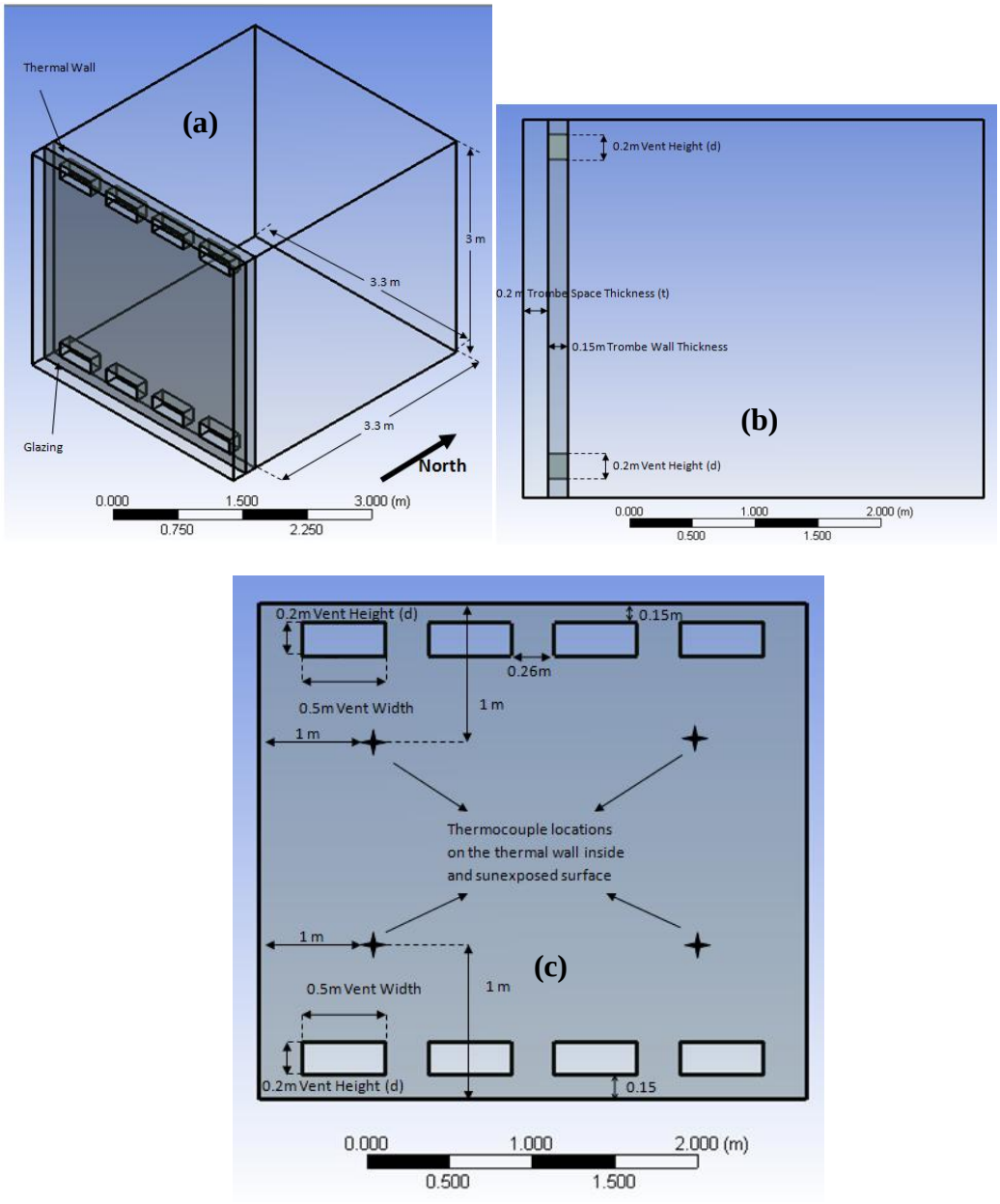

Figure 3.3 : Schematic of the solar house **(a)** isometric view **(b)** east – west (side) view **(c)** south – north (front) view.

Figure 3.3 (a) shows an isometric view of the geometry. Figure 3.3 (b) and (c) shows the side and the front view. The vent height (d) dimension and Trombe space thickness (t) is varied to optimize the performance in Chapter 5.

As the sun exposed solar wall is the main surface for the heat gain, the temperatures are taken on four points on inside and outside surfaces of the solar wall. The thermocouple locations on the thermal wall are seen on Figure 12 (c). The locations are the same for inside and outside surface of the thermal wall. A total of 8 thermocouples are used on the wall.

There are also 4 thermocouples on the glazing. Two of them measure the temperature on the outside while 2 of them is in the inside surface of the window.

The main space has one thermocouple for all free walls, which are East wall, North Wall, West wall, Roof and floor. Also one additional thermocouple measures the temperature at the midpoint of the room. This is accepted as the temperature of the room.

3.2 Measurement Results

The data are collected for the time range 13:20 – 05 –April -2013 to 16:40 – 12 – April -2013. The temperature variation throughout the whole time domain on the solar wall and windows is seen on Figure 13.

Dates 5-6-10 April are sunny days while, 7-8-9-11 April are very cloudy days. Figure 3.4 shows the ambient exposed surface and inside surface of the windows. A slight difference is observed between them, which are caused by the windows transparency effect. Also very dense fluctuations of temperature are observed on the window temperature. (b), in Figure 3.4 shows the average temperature change in the observation time range on inside and sun exposed surfaces of the thermal wall. An observation is that the inside surfaces of the thermal wall follows the trend of the sun exposed surface at day times. But at heating peak times, which are afternoon, the heating effects the inside surface slower. Also it is possible to see that in the nights of the cloudy days, the sun exposed face is cooler than the inside surface. This is because of the heat storage effect of thermal wall. The stored heat in the day time is given out at nights. The sun exposed face is more open to the ambient conditions

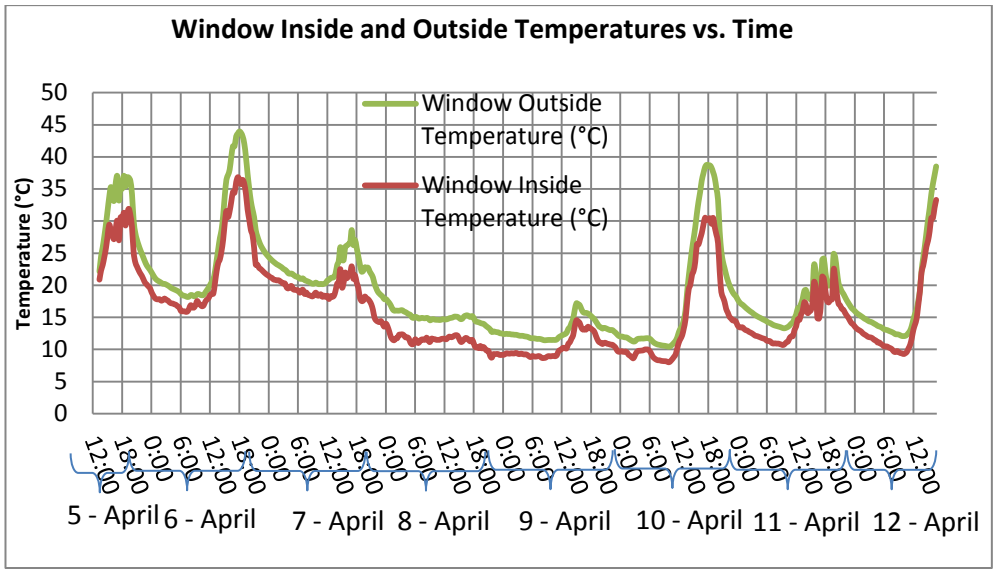

(a)

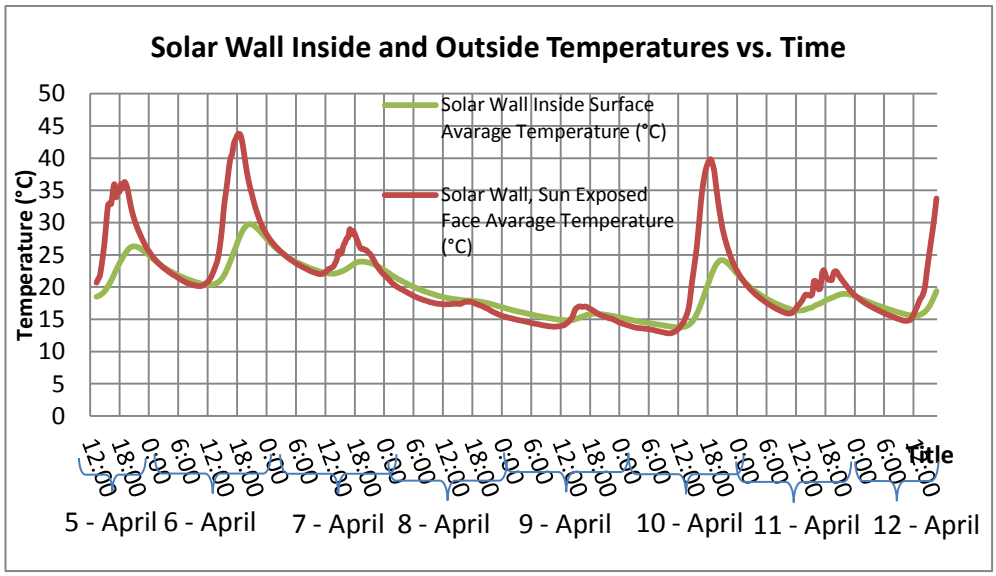

(b)

Figure 3.4 : Solar wall temperature variation **(a)** window inside and outside temperature **(b)** solar wall inside and sun exposed surface temperature.

A shading or insulation that would only work at nights would slow the heat loss rate at night, thus using the thermal wall more efficient. Another observation is that the fluctuations of the temperature graph of the windows, and the sun exposed thermal wall surface. These fluctuations are not observed on the inside surface. This shows the damping effect of the wall.

The temperature curves on the inside surfaces and the main space midpoint are seen on figure 3.5.

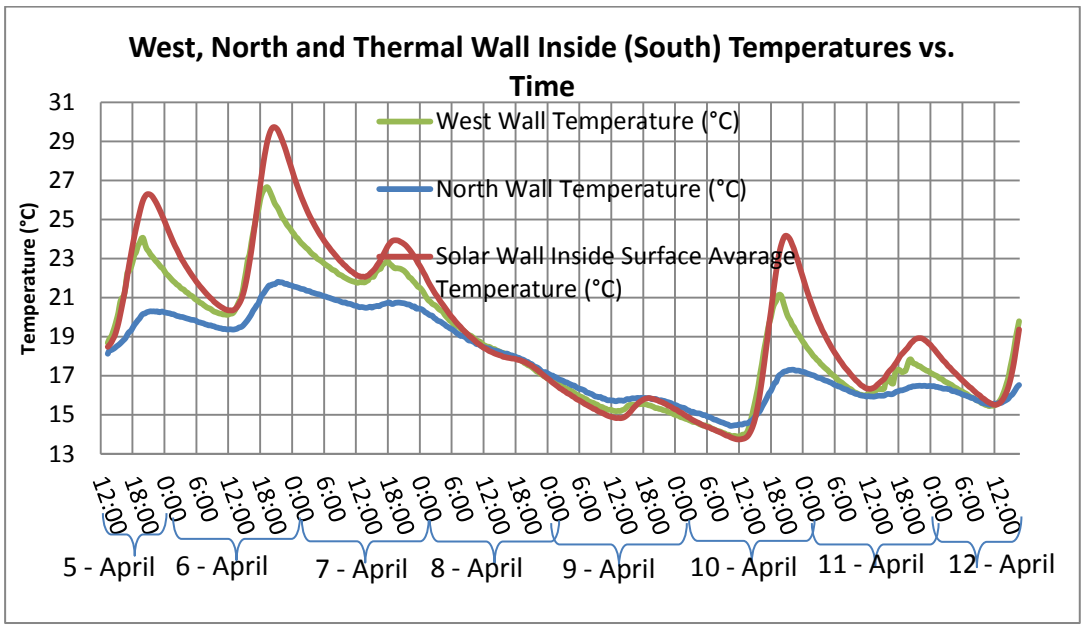

(a)

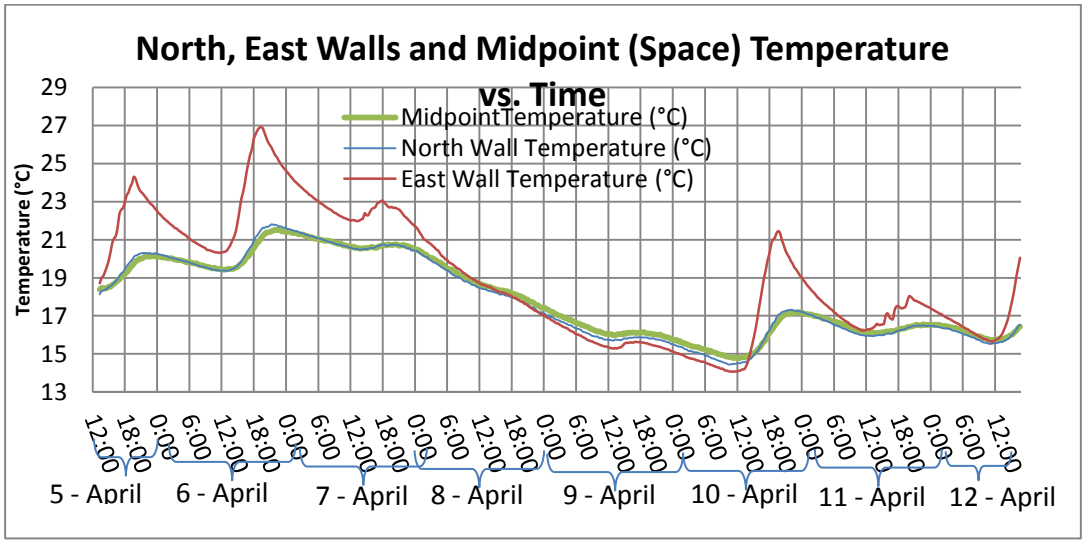

(b)

Figure 3.5 : Measured temperatures vs. time **(a)** the north, east and west wall **(b)** midpoint and thermal wall inside surface.

As seen from Figure 3.5 the hottest wall is the thermal wall inside wall. The heat is conducted from the Trombe wall to this surface. Some of the heat is circulated by free convection with vents. The aim is to increase the midpoint temperature. For this purpose, CFD will involve.

These measurement results will be used to estimate the error of the CFD analysis, in the following chapters.

4. BUILDING ENERGY SIMULATION

4.1 BES Fundamentals

Building energy simulation (BES) programs can provide hourly information about buildings' heating and cooling loads. Lately, BES programs have been used widely for predicting a building's energy consumption. These calculations are even used for legal construction permissions. The accurate calculation of the energy consumption is becoming more important.

BES software can give very accurate results for simple building schemes. Also, BES are available for successfully calculating average space temperatures with special algorithms for studies like this.

The most widely used building energy simulation software is the EnergyPlus code. It is the basic code for most of the energy modeling software such as eQuest, DesignBuilder etc.

In this study, EnergyPlus is used for the BES calculations.

EnergyPlus is a collection of many program modules that work together to calculate the energy requirements of a building. It simulates the building's heat gain and loss, energy systems demands. The simulations are based on fundamental heat balance equations. The time domain is given by the user for the simulation. It can give results for specific time intervals as well as in a whole year domain [27].

The essential variable for this study is the solar heat gain of the solar wall. This depends on the solar radiation levels. Even if the solar irradiation values are known, it is a challenge to calculate the solar wall heat gain from this. The heat gain of the solar wall is calculated with special algorithms of BES. EnergyPlus also has a weather data for Istanbul. This data includes solar radiation, sky clearness average values for calculation.

The weather data is an average data for the region. It does not necessarily match with the real situation in any year but an average for the location.

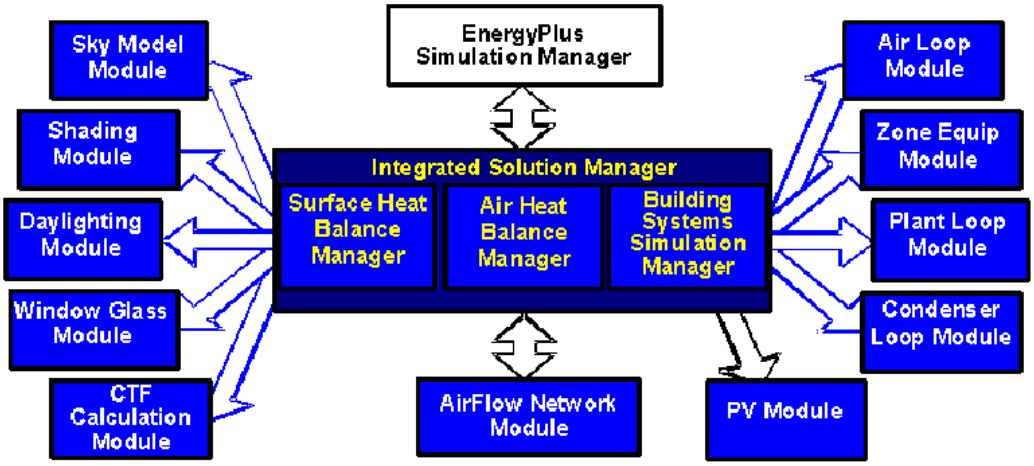

Figure 4.1 : Energy plus program schematic [27].

Figure 4.1 shows the Energyplus software schematic. The solar wall problem requires the solar heat gains to be calculated in detail. Sky Model Module, Shading Module, Daylighting Module and Window Glass Module are used in this calculation. The working of all of them together makes it possible to calculate the heat gain for the Trombe wall.

Next section is a summary of the basic algorithm behind these calculations.

4.2 Solar Radiation and Heat Gain Calculations

The solar radiation is calculations are based on the weather data. The radiation values are taken directly from this file.

The solar radiation has two components. Direct solar radiation and diffuse solar radiation.

The splitting of direct and solar radiation values from a total radiation value is done using the Perez model. [27]

The study about diffuse and direct solar radiation calculations study made Perez in 1992[28] states that the solar radiation can be splitted to direct and diffuse sky radiation as follows;

$$G = Bcos(\Theta) + D \quad \textbf{(4.1)}$$

Where G is the global radiation, B is direct beam radiation, Θ is the incident angle and D is diffuse sky radiation.

The global radiation is experimentally determined. The ratio of D to B, is calculated with a series of correlations that include dew point temperature. The dew point temperature is a good measure of the water contamination in the ambient. Also sky clearness factors are calculated and measured according to several parameters, including visible radiation situation.

The diffuse sky radiation is calculated using ASHRAE clear sky solar model. The mathematical details of this model can be found in [29].

The heat gain of a surface arising from the incident radiation is calculated using the daylighting module. This module calculates the view factor of the surface to the radiation sources, the direct beam and diffuse sky radaitions. The shading of external objects, the reflected radiance from the surrounding objects and ground are also taken into consideration. The glazing transmittance is also an important parameter. All these parameters are taken into account in an iterative approach for finding the solar heat gains of a surface in BES.

4.3 EnergyPlus Calculations

The geometric model for the energy plus is very simple. The walls are modeled with zero thickness. The model is divided in two zones. One is for the Trombe space, between glazing and the solar wall and the other is the main space. The names of the zones and walls which will be used on all the calculations are shown with the EnergyPlus geometry on Figure 4.2. The solar house heat gain is a complicated problem. BES calculates the building heating parameters with a zonal approach. In the figure 4.2, a very important difference from the actual geometry is observed at first sight. The vent geometry is different from the actual one. As the EnergyPlus cannot calculate the exact air flows, vent geometry is not important. It calculates the heat and mass transfer between zones based on the vent size only. The buoyancy and flow effects are not modeled in detail. So it is not needed to model the vents exactly in shape. The real flow situation will be calculated later.

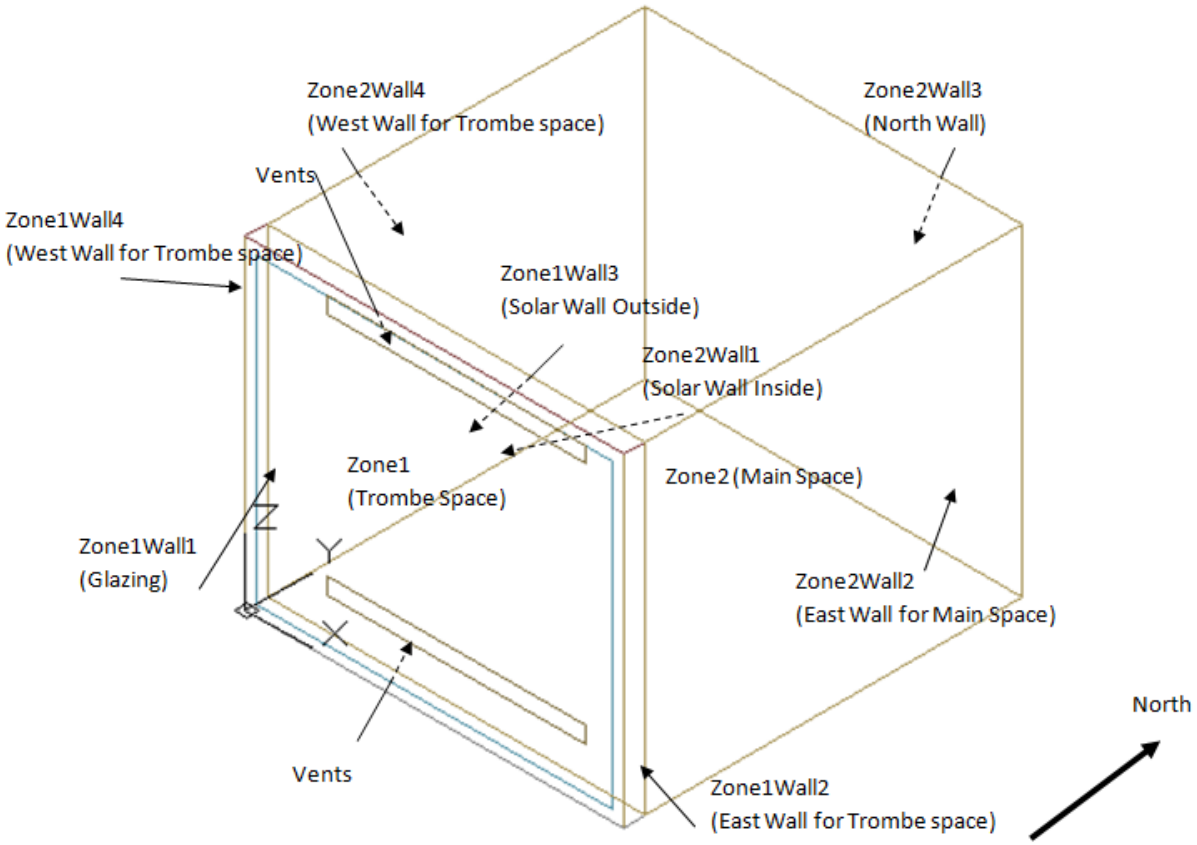

Figure 4.2 : EnergyPlus calculation geometry.

The EnergyPlus simulation has been run for two conditions, winter and spring.

The winter condition is for 01 February 01:00 – 03 February 00:00 and the spring condition is chosen as 05 April 01:00 – 08 April 00:00. The weather data for İstanbul includes the solar irradiation and outside dry bulb temperature data for these days. The distribution of solar data and outside temperature for these two cases are seen on Figure 4.3 and Figure 4.4.

In these randomly chosen days, for the winter case; February, it is possible to see two low solar radiation days and one day in which solar heating is relatively high. This should give the possibility to observe the heat storage effect of the thermal wall and the usage of stored heat in a cold day. For the spring condition, the third day is also with low solar radiation rates. With this the thermal storage effect will also be assessed for spring condition.

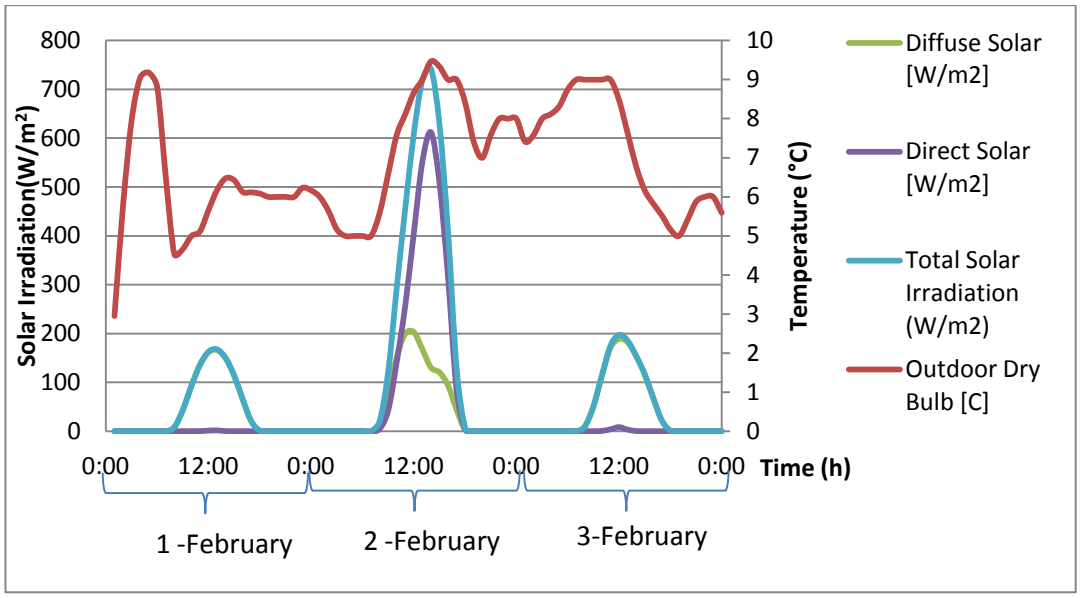

Figure 4.3 : Solar irradiation and outdoor temperature data on winter condition (01 Feb – 03 Feb).

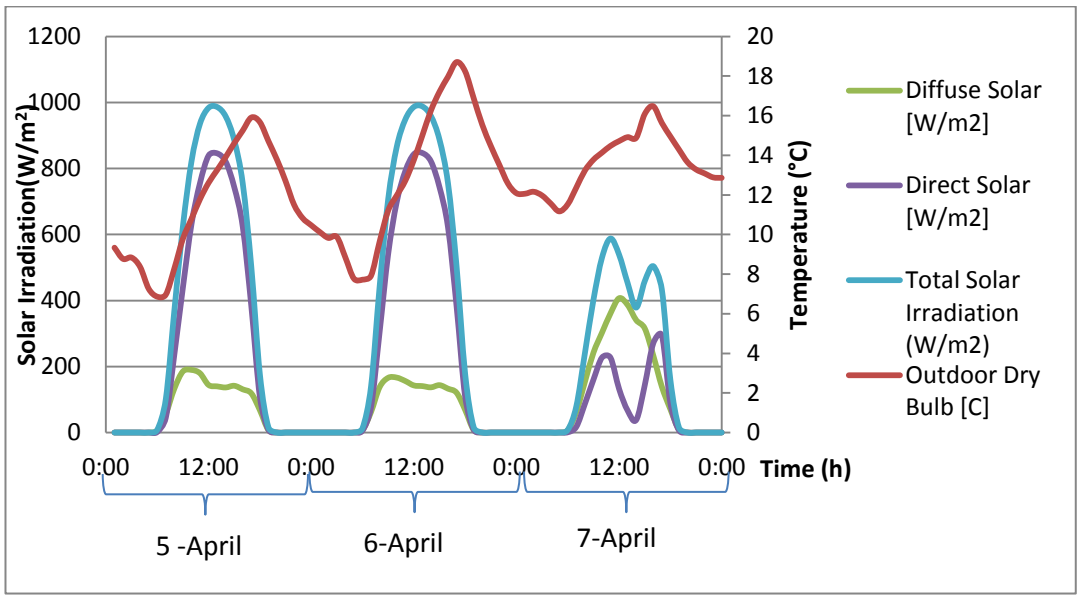

Figure 4.4 : Solar irradiation and outdoor temperature data on spring conditions (05 Apr – 07 Apr).

As mentioned earlier EnergyPlus is used for calculating the heat loss and heat gains. The solar wall heat gain is the main parameter for CFD time dependent calculations. Instead of geometry, the solar wall heat gain, mainly depend on surface absorbtivity properties.

The total heat gain of a surface is determined by the solar irradiation rate and the emissivity of the absorber material, which in this case is the thermal wall sun

exposed surface. For higher ε, one expects to obtain higher values of solar wall heat gain.

The ε value is varied to see this effect. The calculation cases are for brute concrete which has an average emissivity of ε= 0.65. The same case is calculated for various ε values. Physically, it is possible to increase ε values using special paints or selective surfaces. This calculation is made for winter dates which are in between 01.02 – 03.02

Figure 4.5 shows the effect of introducing different ε values to the solar wall heat gain rate.

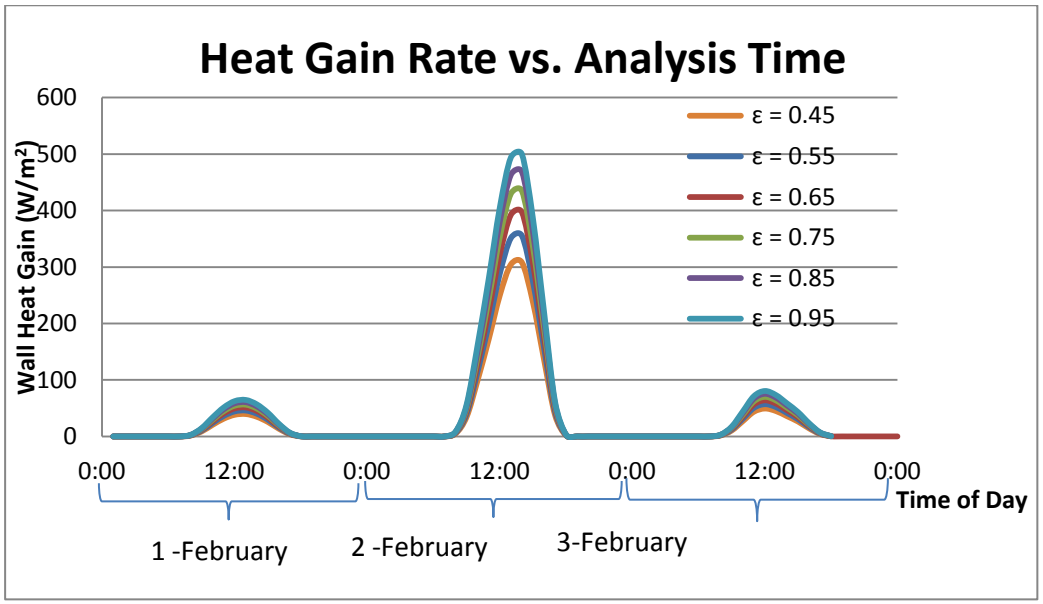

Figure 4.5 : Thermal wall sun exposed surface (Zone1Wall1) heat gain for different ϵ values.

As expected, the wall heat gain rate increase as the ε value is increased.

The calculations from BES will be used as boundary conditions to CFD analysis. A moderate value of ε = 0.65 is chosen for all calculations. The main output of the EnergyPlus calculation is the average temperature of the main space (Zone 2). Its deviation for a moderate value of ε= 0.65 is seen on Figure 20.

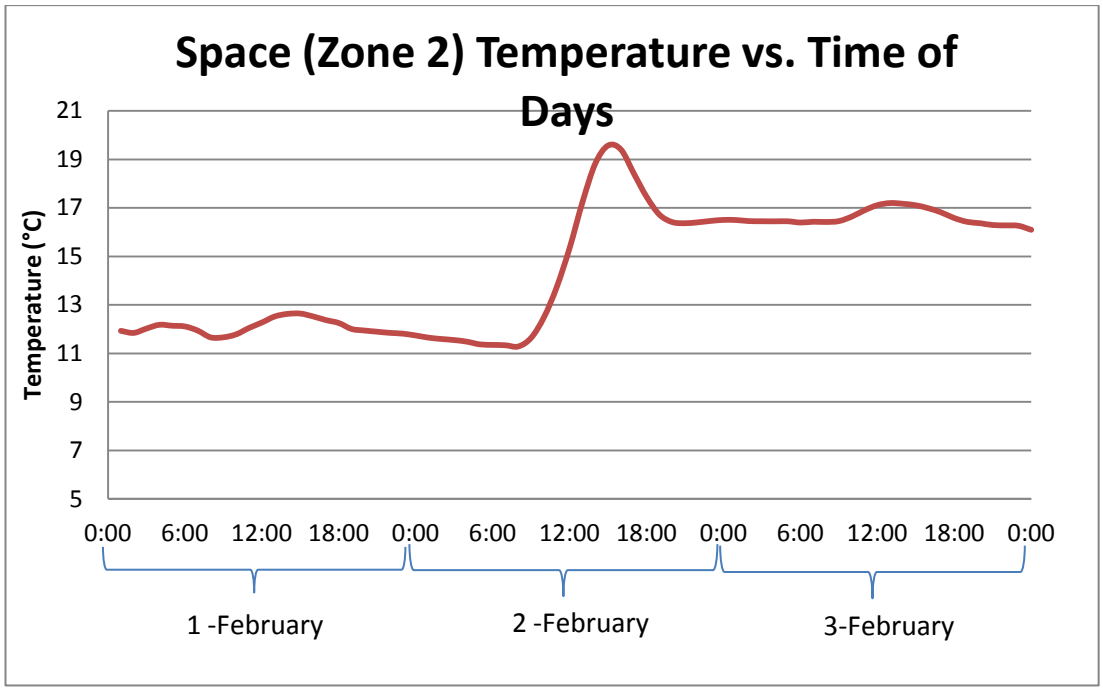

Figure 4.6 : Zone 2 temperature vs. time.

The temperature variation seen on figure 4.6 is an approximate temperature variation and it can be accepted as true. But, as any BES software, EnergyPlus cannot take the flow dynamics issues into account. It calculates the heat balance between two zones according only to the opening sizes. For a problem like a vented thermal wall, it would not be reasonable to try to optimize the Trombe wall parameters. Despite its advantage on solar heat gain calculations, the Zonal approach would be unsatisfactory for optimization of the wall. For optimization, a more complicated tool, Computational Fluid Dynamics can be employed.

The parameters to be used in CFD calculations as boundary conditions that are outputs of the EnergyPlus simulation are; a) radiation heat gain rate of solar wall, b) heat loss of the glazing.

5. CFD MODELING

For understanding the flow behavior inside the occupation space and Trombe space, CFD analysis has been made. CFD modeling will be used to determine the convection effects driven by buoyancy. A better prediction of heat transfer is aimed.

5.1 Overview of the Method and Study

For CFD modeling of the problem, the commercial CFD software package Ansys CFX is used. For geometry editing, the geometry module of Ansys, Design Modeler is used. For meshing, Ansys Meshing Software is used.

CFD is a numerical, iterative method for fluid dynamics problems. It uses a finite number of volumes that the solution domain is divided into. These finite volume elements are called “Cells” and the final grid of these cells is called “Mesh” or “Numerical Grid”. There are different terms for these concepts that can be found in literature.

CFD Software solves the Navier – Stokes equation for fluid movement and Energy Equation for the heat transfer. These equations are solved for each finite volume and the results on the boundaries and the centers of the cells, are interpolated via schemes coded in the software.

For a CFD simulation to be correct, the mesh must be appropriate. More important from the mesh, the definition of the boundary conditions for the solution domain and the physical models must be correct. The nature of the boundary conditions and physical models used in this study are explained in the following section.

There are several models and boundary condition types’ definitions in this software which are explained in detail.

The vent places and sizes would change the heat gain and performance of the solar wall.

The Trombe wall space has been investigated to find the best configuration and the best possible air flow distribution in the heated space. It is aimed to find the most efficient configuration.

The only simulated side of this analogy is the room air. This solution gives the wall convection heat transfer coefficient h_w, inside wall temperatures, $T_{w,i}$ and the room air temperature. For occupant comfort, room air temperature Ti is the main parameter. In all the calculations, it is aimed to keep the room average air temperature, T_i as high as possible.

For different configurations of the solar wall, k_{wall}, T_a and h_a is kept constant. So, T_i only depends on the wall inside convection heat transfer coefficient. As the heat gain of the solar wall moves the inside air by buoyant forces, this motion affects the convection heat transfer coefficient. As the velocity increases near a wall, h_{room} value will also increase. But also, as the velocity near the heat source Trombe wall affects h_{tr} and affects the efficiency and benefit from the absorbed heat by the solar wall. So there is a combined effect of parameters effecting the room air temperature for a trombe wall design. These are;

- The heat gain rate of the Trombe wall
- The flow profile inside the Trombe space
- The flow profile inside the occupied room

These parameters depend on below parameters;

- The geometry and orientation of the solar wall
- The absorber material of the solar wall
- Thickness and volume of the Trombe space
- Trombe wall vent sizes and places

In this thesis, geometrical aspects of a passive house with a Trombe wall will be investigated with CFD Analysis

These geometrical parameters are, the thickness of the Trombe wall, and size of vents. Also, the thermal wall material is varied. Aluminum, concrete and wood for the thermal wall configurations are simulated to see the effects.

5.2 Physical Models

Computational Fluid Dynamics programs mainly solve the Navier – Stokes equations. Though, for special behavior of the fluids, additional models are required. The most essential of this models, is the turbulence model. Buoyancy model, mixture model, combustion, multiphase models all use different sets of equations. These models basically modify the governing Navier-Stokes equation in order to see different effects on the flow. In this study, a turbulence model will be used to visualize and see the effects of turbulence in the final results. Also, since the air movement is all induced by natural convection, employed buoyancy model will be explained

5.2.1 Turbulence

For a building interior flow, though the velocities are low, it is possible to observe turbulent flows in some locations. The turbulence level is known to increase the convection heat transfer coefficients. An example for this phenomenon can be seen on Figure 5.1. The turbulence in a rectangular cavity higher Reynolds numbers increases the Nusselt number.

Where

$$Re = {V.D_h}/{\upsilon} \quad \text{and} \quad Nu = h_f.L \,/\, k_f \,, \tag{5.1}$$

as mentioned before.

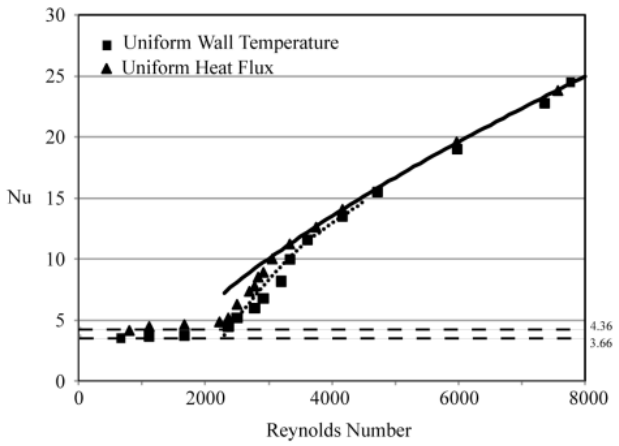

Figure 5.1 : Nu vs. Re numbers for a rectangular Cavity [30].

If Reynolds number is bigger than 2300, the flow is said to be in the transition zone to turbulence for an internal flow. Figure 5.1 shows the dramatic change in Nusselt number as the flow enters the turbulence zone. Increasing Nusselt number increases heat transfer coefficients. So, even if the velocities are low and a high level of turbulence is not expected, turbulence must be solved in order to determine heat transfer correctly since there is a possibility of turbulence in small Reynolds numbers in the solar house problem.

In this study, the Trombe space geometry and the vents are rectangular cavities; also it is possible to see turbulence effects on the free walls surrounding the main space. As the turbulence affects the convection heat transfer coefficient strongly, it cannot be ignored.

There are several approaches for solving the turbulence. One approach is k - **ϵ** model with wall functions, this approach is explained in next section.

5.2.2 k-ϵ model

This turbulence model has been implanted in several CFD solvers as it is considered as an industry standard model. This model has been used for this study.

The k-ϵ model simultaneously solves the "k", the turbulence kinetic energy and **ϵ,** the turbulence dissipation rate.

To understand the results of the turbulence parameter output of the simulation, k; the turbulent kinetic energy, should be understood.

Turbulence can be visualized as the deviation of the instantaneous velocity and pressure from the time averaged velocity for an observed point or region at a given time. In other words, a turbulent flow is a fluctuating flow when observed. This fluctuation is random and chaotic. The real situation cannot be solved analytically for a turbulent flow, but models can be used to accurately estimate the level of this fluctuation. The other parameters such as convection heat transfer coefficient depend on the level of this fluctuation.

Turbulent kinetic energy is a measure of the deviation of the real velocity from the time averaged velocity. This model solves this variable. As seen on figure 5.2, the magnitude of the deviation is the u'. u is the velocity vector in one direction, x. The

other direction and velocity components should have the similar behavior. As the nature of the definition, the time average of the u' must be zero.

$$\overline{u'} = 0 \qquad \textbf{(5.2)}$$

For understanding the time averaged fluctuating magnitude of the turbulent flow, RMS of this time average is taken, which is $\overline{u'^2}$. If $\overline{u'^2}$ =0, then the flow is laminar (no Turbulence). If $\overline{u'^2} \neq 0$, the flow is turbulent and the magnitude of it is a measure of the turbulence level.

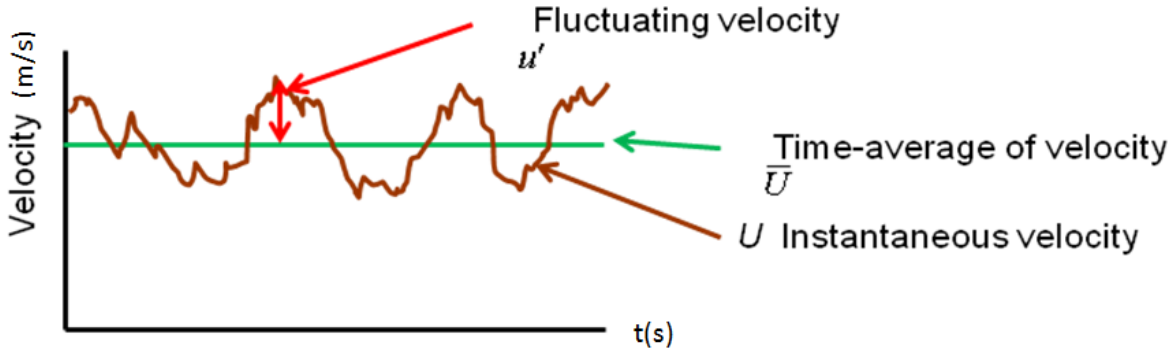

Figure 5.2 : Velocity and fluctuating velocity definitions for turbulence.

"k"; the turbulence kinetic energy is defined as a measure of fluctuation in all 3 directions as;

$$k = 0.5 * \left(\overline{u'^2} + \overline{v'^2} + \overline{w'^2}\right) \qquad \textbf{(5.3)}$$

in terms of, m^2/s^2

Another measure is for the turbulence is ϵ, turbulence dissipation rate. This variable is the measure of the rate turbulent kinetic energy that is converted into thermal energy, thus dissipated as heat. The unit of the term is m^2/s^3. This value is an important variable for the flows that viscous heating is an important parameter. For the solar house flow case, as the velocities are small, the heating effect is not important. The dissipation rate of the "k" must be calculated in order to find the ending location of turbulence of a flow in a specific region.

5.2.3 Buoyancy model

In the solar wall problem, only inductance of flow motion is the buoyancy due to the temperature differences. The buoyancy should be solved adequately to observe the realistic flow parameters.

The buoyancy simply is the movement of the lighter fluid above the denser fluid. For a one phase domain, like the solar wall problem, only gaseous air, the decrease in density which moves the fluid is provided by the temperature differences. This is called natural convection. The air motion in a cavity with constant temperature walls one of which is lower than the other can be seen on Figure 5.3. As seen on figure, as the temperature increases, the motion is against the gravity. This is because of the decrease in density.

For modeling this movement a model, Boussinnesq is used in CFX.

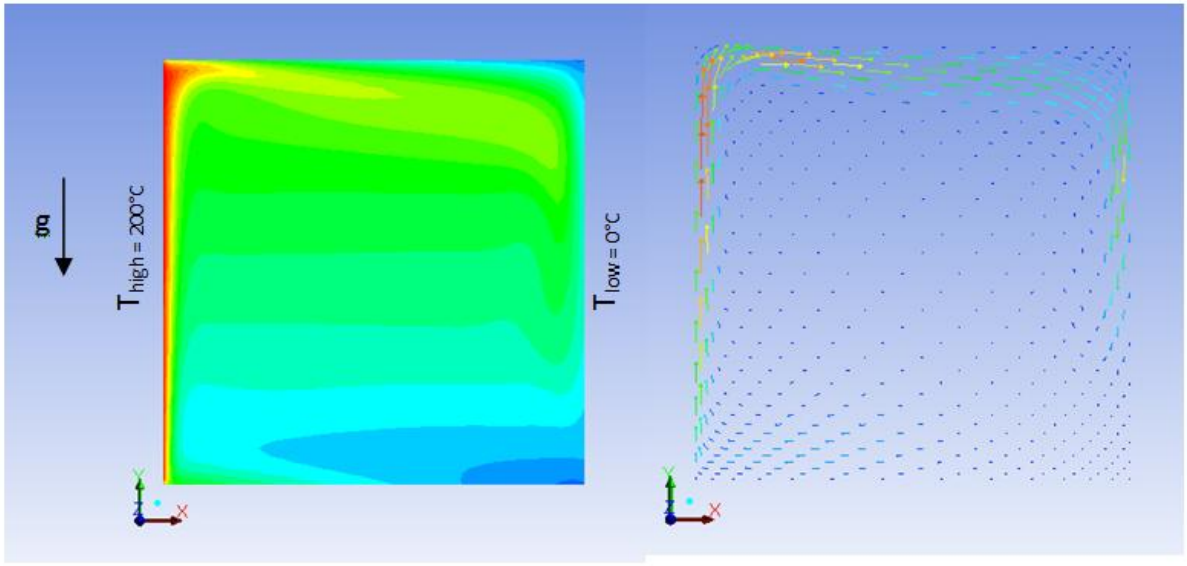

Figure 5.3: A natural convection example in a square cavity **(a)** Temperature contours **(b)** Velocity vectors.

The buoyant force on a fluid particle is determined with its density, a reference density and gravitational acceleration. For a buoyant flow

$$F_b = g(\rho_f - \rho_{ref}) \quad \textbf{(5.4)}$$

Where F_b is the buoyant force on the fluid, g is the gravitational acceleration, ρ_f is the fluid density and ρ_{ref} is the reference density. Solving this equation requires the solving of the density in CFX. This would require additional computation power. For more accurate solutions flows with small differences "Boussinnesq model" is advised by CFX- User Guide [31]. Using this model decreases the computational power need. One more advantage is, it is directly using the Temperature difference,

thus easily couple forces with energy equation to solve the natural convection heat transfer more accurately, increase robustness, and i.e. makes the problem easier to converge. In Boussinnesq model, buoyancy force equation is reduced to;

$$F_b = -g\beta\rho_{ref}(T_f - T_{ref}) \quad \textbf{(5.5)}$$

Where, ρ_{ref} remains the reference density, T_{ref} is the reference temperature and β is the thermal expansion coefficient for the reference temperature. The thing that special caution must be held using this model is to determine the reference temperature reasonable. It must be an average temperature for the whole domain. All the buoyant force should sum up to the 0 in the converged solution. Choosing a reference closer to the average will decrease the convergence time of the simulation.

As the flow motion is induced by buoyancy only in the solar wall problem, specific caution has been held for the buoyancy model input values such as reference values.

5.3 Boundary Condition Types;

For configuring a CFD simulation, the boundary condition in all necessary locations must be defined very carefully. For this study, there are no flow inlets or outlets, but only thermal boundary conditions. The nature of these boundary conditions must be understood clearly in order to define them right. This section explains the necessary boundary conditions for the solar house problem.

5.3.1 Heat transfer coefficient and outside temperature (Drichlet)

In this boundary condition type, required data is a heat transfer coefficient and the outside temperatures.

In Figure 5.4, the analogy behind the heat transfer coefficient wall boundary condition is seen. q_w is the heat transfer from the non modeled outside ambient and wall for the simulated case.

From the resistor anology in the figure,

$$1 / U_{total} = 1 / hi + dtw / k + 1 / ha \quad \textbf{(5.6)}$$

which can be reduced to;

$$1 / U_{total} = 1 / h_i + 1/U_{out} \quad \textbf{(5.7)}$$

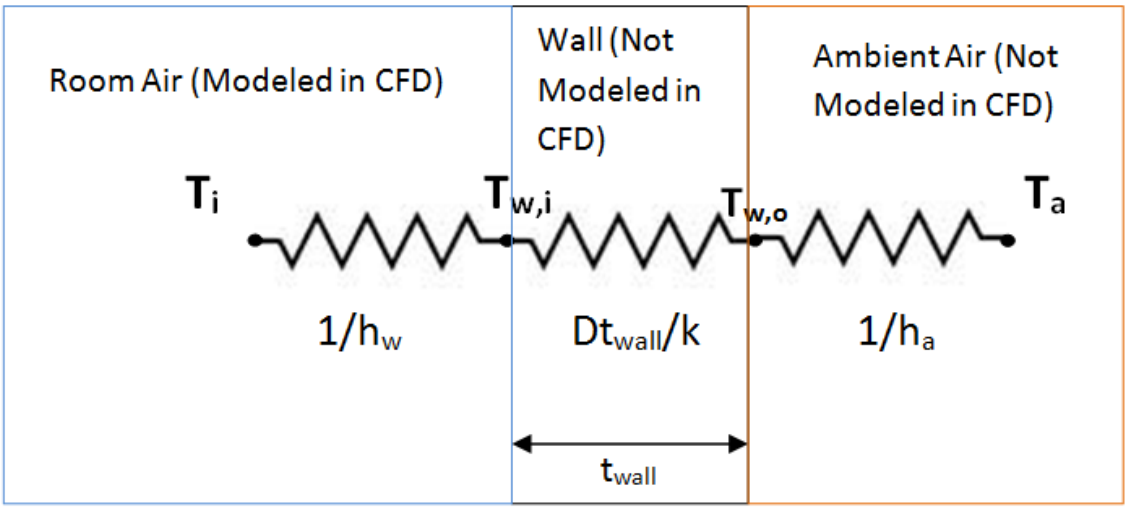

Figure 5.4 : Visualization of the Heat Transfer Coefficient and Outside Temperature Boundary Condition.

U_{out} term should be defined as the heat transfer coefficient for the boundary condition. Combining *(5.6)* and *(5.7)*;

$$1/U_{out} = t_w/k + 1/h_a \quad \textbf{(5.8)}$$

Equation 5.8 simply combined wall conduction heat transfer coefficient which depends on the material and wall outside convection coefficient which depend on wind speed and turbulence situation.

For a reasonable, constant approximation of these values, ASHRAE resources are used.

ANSI/ASHRAE Standard 62.2-2004 [32] advices heat transfer coefficients for outside the building as 34 $W/m^{2}.K$. This value is accepted as h_a. For the wall thermal conductivity, a concrete wall is considered. A k_w value of 1.4 W/m.K is accepted. The wall thickness, $t_{w,}$ is accepted as 0.04 m for this calculation. When U_{out} in equation 5.8 is solved for these values; U_{out} is calculated as 17.24 $W/m^{2}.K$.

As U_{out} value increase, heat flux from the room air to the outside ambient will increase. For observing the differences between the solar wall configurations, an avarage value of U_{out} which is 20 $W/m^{2}.K$ is used for the free walls that are assumed to have no solar heat gain.

5.3.2 Constant temperature wall boundary condition

One more boundary condition which is used in CFX is the constant temperature boundary condition. This boundary condition is based on keeping a domain wall in

constant wall temperature and the heat transfer between the wall and the fluid is determined using this wall temperature and the adjacent cell temperature. The convection and conduction effect to the fluid are observed.

This type of boundary condition is used in experiment simulation CFD analysis and for the floor temperature for all the simulations

5.3.3 Heat flux

The heat flux from the wall to the fluid is determined by a constant heat flux value in terms of W/m^2. A positive value indicates heat flux through the fluid while a negative value indicates the heat flux from the fluid to the walls. This type of boundary condition is used for the solar wall heat gain and heat losses from the glazing in several simulations in the study.

5.4 CFD Study

For geometry optimization, 2D and 3D methods of CFD is used. For determining the flow patterns and 3D effects on velocity, air temperature distributions, steady state 3D CFD analysis has been made with Ansys CFX software**.**

Though a 3D model shows the velocity and temperature distribution, it is not practical for an hourly, time dependent calculation. As the effect of the solar wall continues throughout the night and the daily temperature is strongly dependant on the solar heat gain rate changes on the Trombe wall. To see the night and solar radiation dependency effects a 72 hour time dependent model has been solved. The boundary conditions are taken from the BES calculations that have been discussed above.

Calculating this time dependent situation would require enormous amounts of computational power and time. As one purpose of this study is to present a practical method for solar wall optimization, the time dependent hourly model is calculated with 2D mesh.

5.4.1 Transient Model – 2D

5.4.1.1 Geometry

Several assumptions and simplifications are made for reducing the 3D flow into 2D. First assumption is that in the actual case; the vents have a finite length. This means the top and bottom vents are a combination of finite length vents. The spaces

between vents are ignored in the 2D case. Also, as the calculation is made on a 2D cross section of the whole geometry. This makes the east and west wall temperatures and heat gain/loss ignored. The reductions and assumptions for the 2D analysis is explained on Figure 5.5.

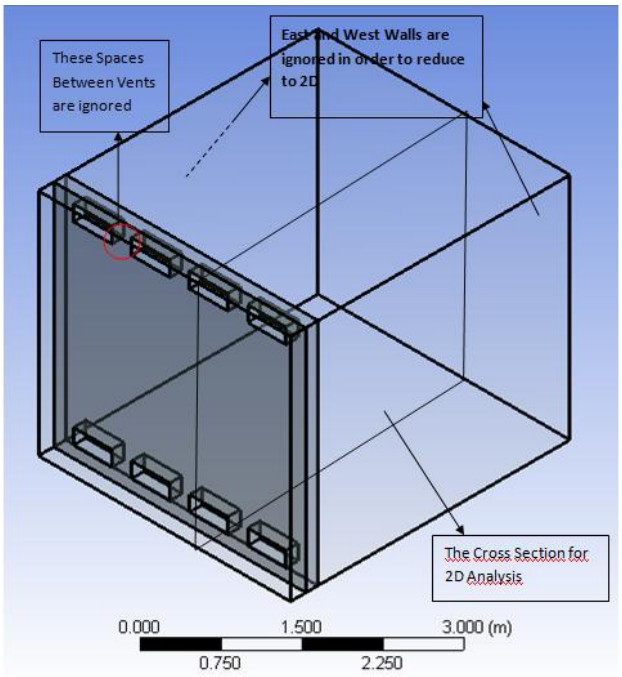

Figure 5.5 : Assumptions and reductions on the geometry.

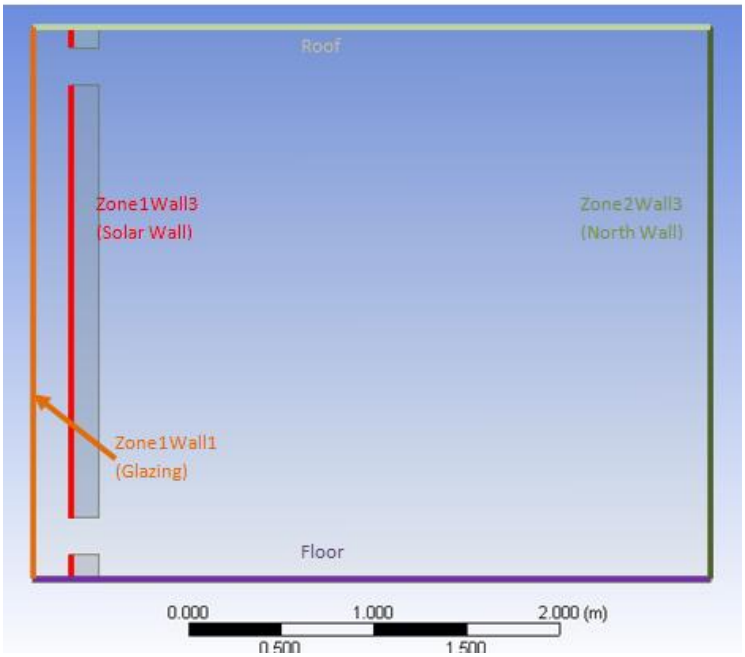

Figure 5.6 : Boundaries on the geometry.

The transient model is used with several boundary conditions for the purpose. The first calculation is made for the real situation boundary conditions.

5.4.1.2 Meshing

For the transient model, a 2D model has been configured. The numerical grid consists of nearly 4000 cells. The exact number differs with configuration.

Also in the flow boundaries i.e. walls, a finer grid has been used for solving the near wall velocity profile

To find a reasonable number of grid elements, a method used widely by CFD engineers "Mesh Independency" is used. This method is used to determine the right amount of elements by trying different mesh structures, from coarse to fine grid. Too coarse grid, meaning less elements, would cause the simulation to calculate the parameters wrong. A too fine grid, meaning increased amount of elements, would cause the computational time required unnecessarily long. To find an optimum mesh size for right solutions and moderate computational times, this preliminary analysis is made.

Table 5.1 : Element number and corresponding domain maximum velocity and temperature.

Number of Elements	**Max Temperature**	**Max Velocity**
1062	305.795 K	0.32745 m/s
2123	299.463 K	0.45754 m/s
2989	295.331 K	0.47611 m/s
3121	292.212 K	0.50112 m/s
3995	290.112 K	0.51432 m/s
5073	289.997 K	0.52321 m/s

For mesh independency check, the same boundary conditions, 300 W/m^2 for the thermal wall heat gain, 20$W/m^2 \cdot K$ is used for wall heat transfer coefficients. Note these boundary conditions are imaginary to find the mesh independency point. K-ϵ

Turbulence model and Boussinesq buoyancy model has been used. For the 2D case first simulation is made by nearly 1000 elements and increased to nearly 5000 elements, it is observed that the solution did not change too much after 4000 elements line. Table 5.1 gives the maximum velocity and maximum temperature on the converged solution with respect to element numbers.

As seen from Table 5.1. After about 3000 elements for the mesh, the solution does not change significantly. An average element number of 4000 elements are used for the calculations. These results are for the steady – state case.

The 2D study will be made transiently for about 72 time steps. The resulting mesh with approximately 4000 elements can be seen on Figure 5.7. The mesh has finer grid near walls in order to catch the high gradients on the wall boundary profiles arising from the no slip condition better.

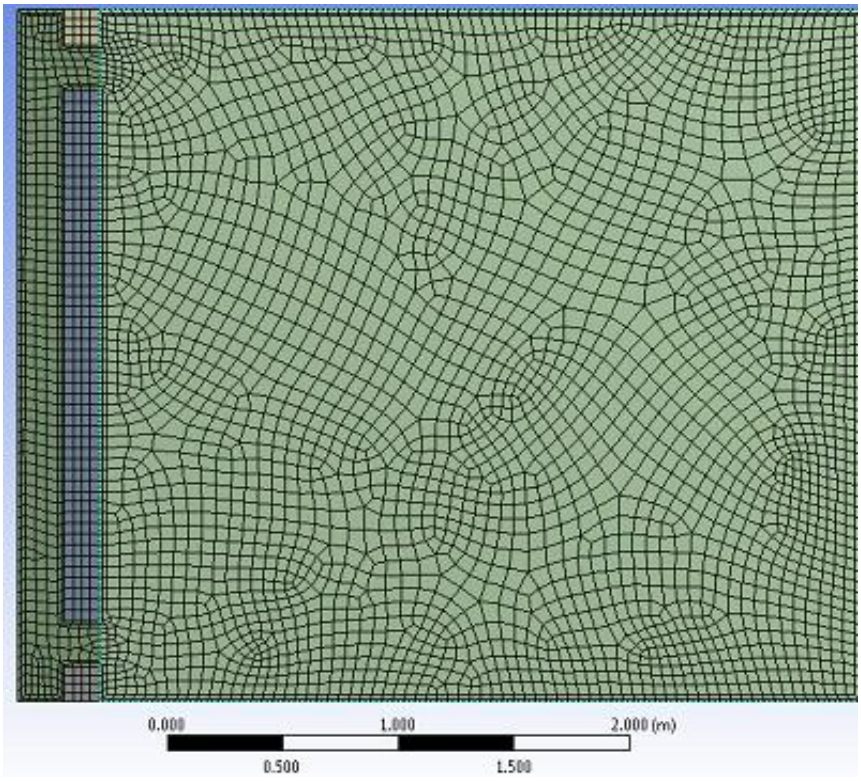

Figure 5.7 : 2D Mesh Structure.

5.4.1.3 Measurement simulation

To validate and find the error that is made with CFD simulation, the real measurements will be compared with the CFD simulation.

For this purpose, the wall temperatures for the 5 day experiment are directly used to simulate the real situations and find the differences of the real situation with the CFD analysis. For this analysis all boundary conditions are constant temperature boundary conditions that change hourly. The experiments results are for 170 hours.

The hourly graph of the constant temperature boundary conditions for all walls can be seen on Figure 5.8. These time dependent boundary conditions are directly taken from the measurement results. The data is the input for the constant temperature boundary conditions of the CFD analysis.

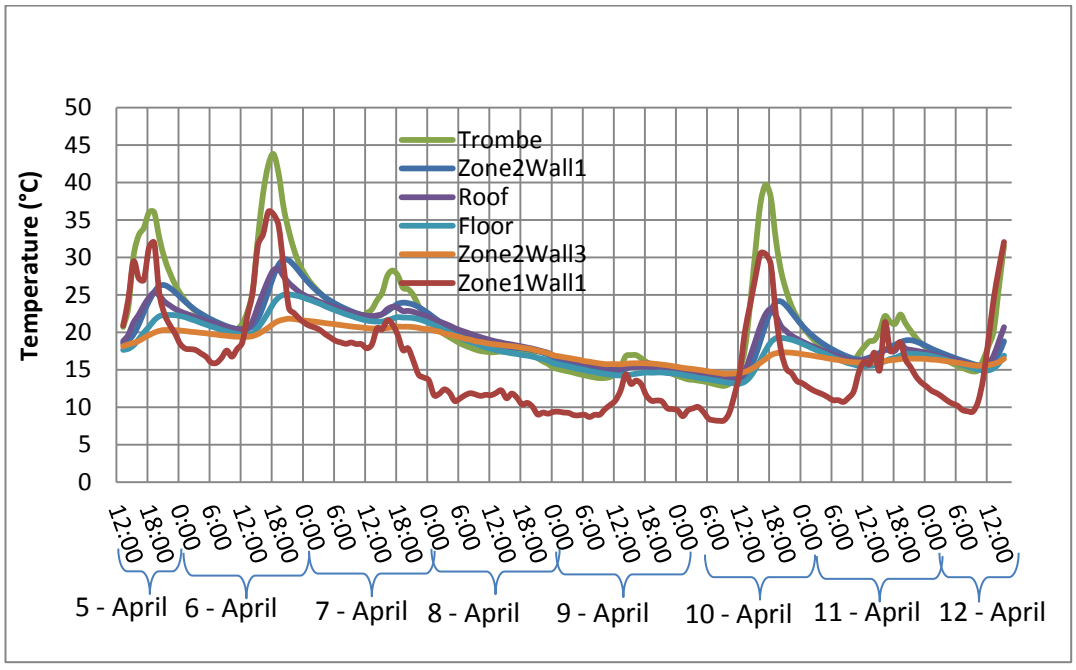

Figure 5.8 : Boundary conditions for CFX 2d simulation for measurement results.

With the models explained above the output of the simulation is the temperature distribution of the spaces. As the purpose is to compare the real situation and the CFD calculation, the comparison between the temperature of a specific point on experiment and the simulation is made. This point is the exact midpoint of the room

The hourly comparison of the temperature as measured in experiment and calculated with simulation can be seen on Figure 5.9.

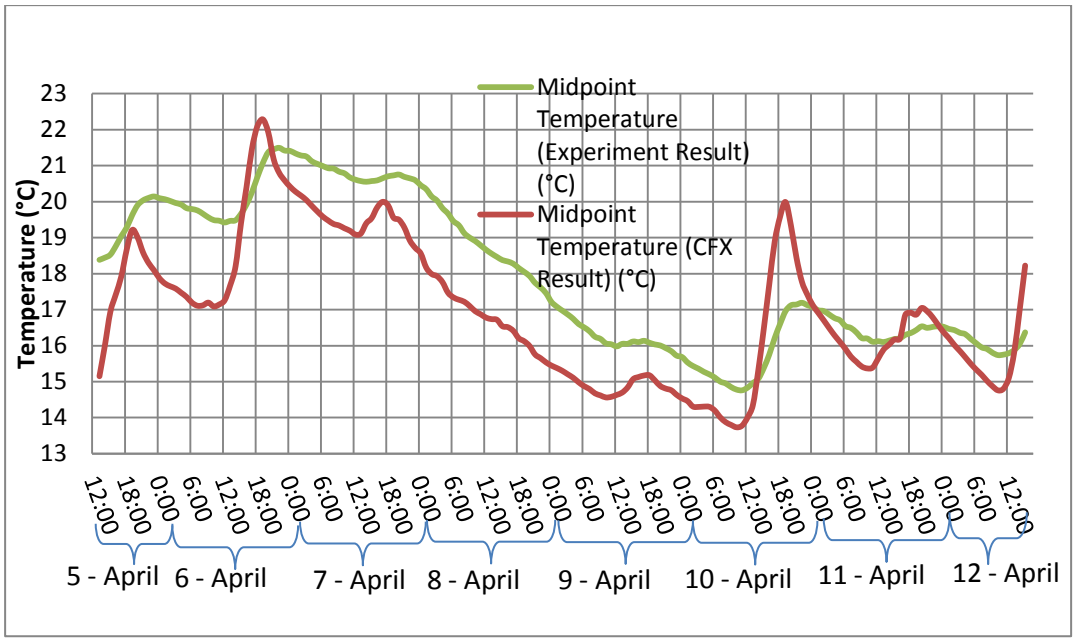

Figure 5.9 : Midpoint temperature for real measurements and CFD simulation.

As seen from the figure, there are slight differences between the experiment and simulation calculations. The most obvious difference is observed on the peak temperature hours which are when the solar radiation is on its peak – afternoon hours. The cooling trends match each other.

Figure 30 shows the per cent differences between these two temperature results. The per cent differences are important to validate the model.

The percent differences are calculated as

$$Percent\ Deviation = |Tmeasured - Tsimulated| \ / \ Tmeasued\ X\ 100 \qquad \textbf{(5.9)}$$

The graph of this deviation can be seen on Figure 5.10. The graph is drawn with respect to data points. These data points represent the time steps, thus hours. The starting data point is 13:20 of 5 April while the end is 15:50 of 12 April.

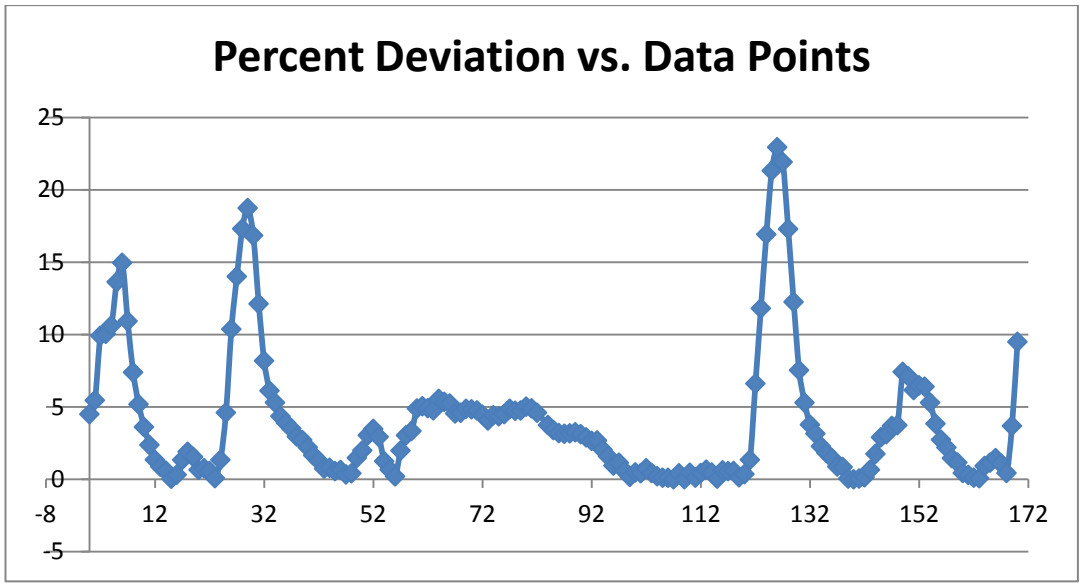

Figure 5.10 : The percent deviation of the simulation results to real measurement.

This trend line in figure 5.10 shows us that in the cooling times such as night and the times with low solar radiation, the error is maximum 5% which can be accepted as a perfect simulation. The problem is on the heating trend line which the difference can be observed on both. Although the trend line of the all deviations barely exceeds %5 at some points, at the heating peaks, deviations as big as 20% can be observed. The calculated temperatures on these points can be considered as overestimated. The reason for this overestimation has several reasons. One is the 2D reduction and simplification which omits the effect of the east and west walls. The second is that in the experiment, there are unexpected and unavoidable air leakages throughout the windows and doors. These effects are not modeled in the simulation. A third reason can be the numerical errors arising from the flow models in CFD and the numerical grid resolution.

The most important difference is that the external walls are not modeled as a numerical grid. Only heat conduction effects of them are considered. The overestimated temperatures are mostly arising from this phenomenon.

With the knowledge of that the CFD simulation overestimates the peak temperatures; this 2D configuration is used for configuration optimization.

5.4.1.4 Case study

CFD will be used for investigating the effect of different parameters on the space temperature and the thermal wall performance. This study can be considered as an optimization for some parameters. This is done by comparing several configurations.

The first configuration comparison is on the trombe space thickness, t. The thickness in the actual case is for 0.2m. 0.1m and 0.3m will also be simulated and the best will be chosen. Another parameter is the height of the vents, which is d. These geometric relations can be seen on Figure 12 (b) and (c).

The cases are seen on Table 5.2.

Table 5.2 : Varied parameters and configurations in CFD.

Trombe Space Thickness (t)	t=0.1m.	t=0.2m.	t=0.3m.	t=0.4m.
Vent Height (d)	d=0.1m.	d=0.2m.	d=0.3m.	d=0.3m.
Materials	Wood	Concrete	Aluminum	

Other than the air flow, the heat is conducted from the heating wall. Also some of this heat is stored in the wall and it is given back to the space at nights. This conduction and storage loop makes the Cp value and thermal conductivity of the solar wall is important for the heat loss/gain balance. These properties are material properties. The real case is for concrete. Also thermal wall materials for wood and aluminum are simulated.

5.4.1.5 Boundary conditions;

For comparing the different configurations, the boundary conditions are determined first. The average temperature in the main space is the output and the subject to comparison between cases.

Different from the previous simulation, this time the boundary conditions are heat fluxes instead of temperatures. The most important boundary condition is the solar wall surface. A boundary source as heat is defined on the solar wall. Also as the heat

transfer coefficient on the glazing depends on many parameters such as radiation intensity, the convection from outside, the window thermal conductivity. These mechanisms have a complicated nature. As an example, at the peak radiation hours, the windows have radiation gains and outside convection losses at the same time. The radiation gains are both from inside and outside but it has a balance with the outside convection heat loss. Also the emission from the glass will be added to the heat losses. Modeling this entire phenomenon in CFD would affect the robustness of the simulation. So certain reductions have been made in order to increase robustness and make convergence easier.

Table 5.3 : Boundary condition types and values for 2D case comparison.

<table>
<tr><th>Buoundary</th><th>Boundary Condition Type</th><th colspan="2">Value</th></tr>
<tr><td>Zone1Wall1 (Glazing)</td><td>Time Dependent Heat Flux</td><td colspan="2">Varies (Figure 5.11 and 5.12)</td></tr>
<tr><td>Zone1Wall3 (Solar Wall)</td><td>Time Dependent Heat Flux</td><td colspan="2">Varies (Figure 5.11 and 5.12)</td></tr>
<tr><td>Floor</td><td>Constant Temperature</td><td colspan="2">10 °C</td></tr>
<tr><td rowspan="2">Roof</td><td rowspan="2">Wall Heat Transfer Coefficient and Outside Temperature</td><td>Wall Heat Transfer Coefficient</td><td>Outside Temperature</td></tr>
<tr><td>20 W/m^2.K</td><td>Varies (Figure 5.11 and 5.12)</td></tr>
<tr><td rowspan="2">Zone2Wall3 (North Wall)</td><td rowspan="2">Wall Heat Transfer Coefficient and Outside Temperature</td><td>Wall Heat Transfer Coefficient</td><td>Outside Temperature</td></tr>
<tr><td>20 W/m^2.K</td><td>Varies (Figure 5.11 and 5.12)</td></tr>
<tr><td>East and West Walls</td><td>Symmetry</td><td colspan="2">-</td></tr>
</table>

The boundary conditions for the roof and the free wall (Zone2Wall3), are a constant heat transfer coefficient. The heat transfer coefficient on CFX is explained in section 4.3.1.

The heat transfer coefficient needs one more value which is the outside temperature. This is also taken from the weather file of EnergyPlus for Istanbul

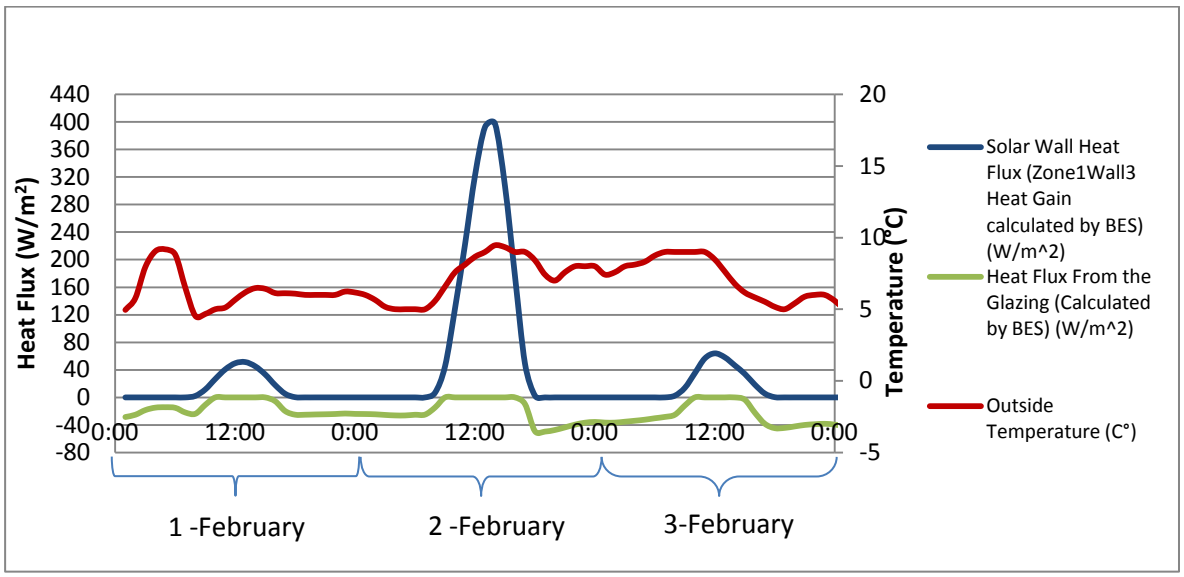

Figure 5.11 : Constant heat flux boundary conditions versus time of days for winter condition simulation time domain (1-3 February)

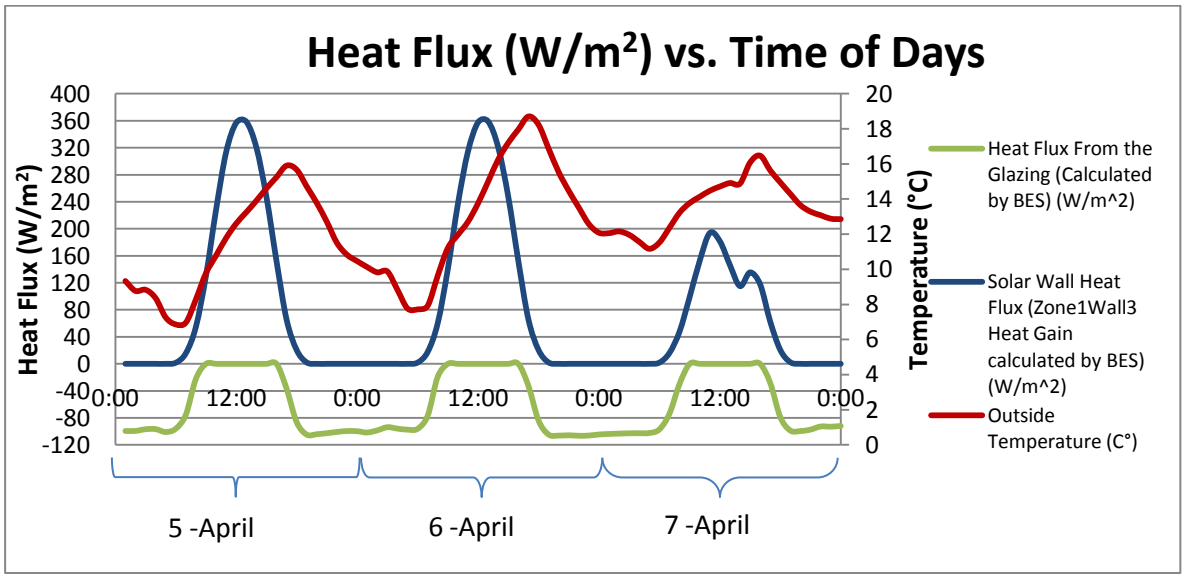

Figure 5.12 : Constant heat flux boundary conditions versus time of days for spring condition simulation time domain (5 – 7 April)

Table 5.3 shows the boundary condition types and values for all boundaries. Figure 5.11 and 5.12 shows the time dependent variation of varying boundary conditions stated in the Table 5.3. All cases are simulated for two conditions of 72 hours; winter condition is for 01 – 03 February and spring condition is 05 – 07 February

As the simulation is time dependent, boundary conditions also are time dependent.

There are two types of boundary conditions, one is constant heat flux, the other is wall heat transfer coefficient with outside temperature. Also a constant temperature of 9 C° is used for the floor.

5.4.1.6. Trombe Space Thickness (t) Comparison Results

The first case comparison is about of the temperature average for winter and spring conditions for different Trombe space thicknesses, Figure 5.13 shows this variation for different Trombe space thicknesses.

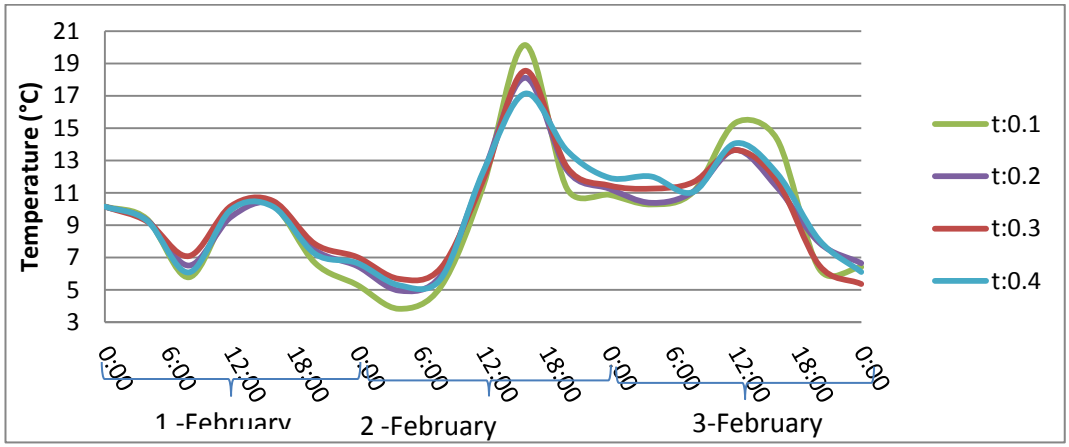

(a)

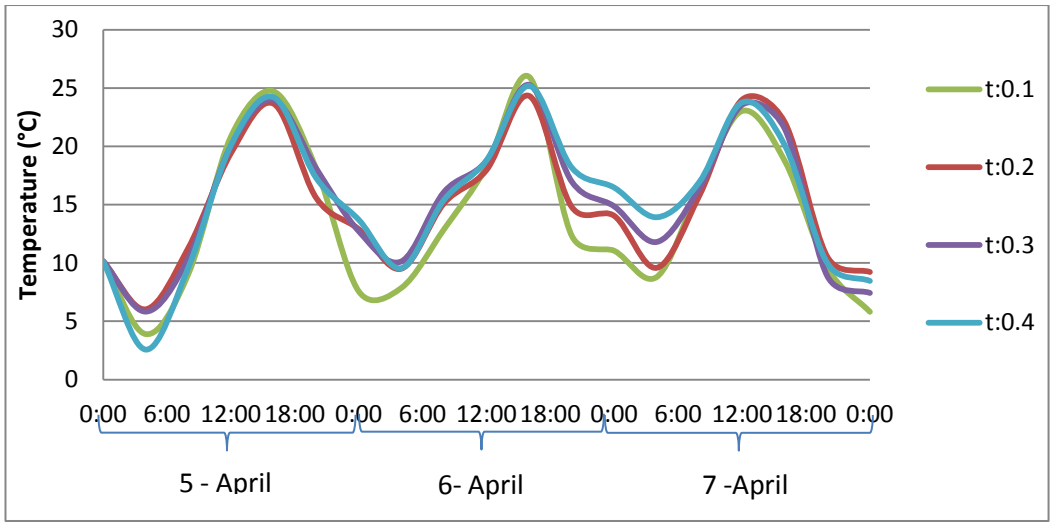

(b)

Figure 5.13: The 72 Hour Temperature Variation of Various Trombe Space thicknesses*(t)* **(a)** Winter Conditions **(b)** Spring Conditions.

The change between the main space temperatures in both winter and spring condition is very little. Though, this little change is important if the energy demand of a big structure should be calculated.

The peak regions of the graph are the solar radiation peaks, where the coolest points are the night when the space begin to lose energy to the surroundings. As seen from both graphs, for the t=0.1m graph, the temperature is higher than the other configurations. This difference is very small. At the night times, as the trombe space thickness gets smaller, the temperature decrease. It can be concluded that the storage ability of the thermal wall gets lower as the space between glazing and the wall decrease. Because the night heating is achieved by the stored heat inside the wall. This should be because, as the thickness increase, the air mass between glazing and the wall increase. This provides an insulation. The glazing has the highest heat loss rates at nights.

5.4.1.7. Vent opening height (d) comparison results

As mentioned, another comparison is for (d) the height, thus the size of the vents. As the vents get bigger, the thermal mass of the Trombe wall gets smaller. But also, the flow resistance from the Trombe space to the main space decrease as it gets bigger.

The figure 5.14 shows the temperature variation for different vent heights. The graphs show a little higher temperature for d=0.1m case at the peak heating times. As the flow inside the main space accelerates, the more resistance it will face when flowing from the Trombe space to main space. That makes a slower flow in the main space, thus lower the heat transfer coefficients causing a decrease in the heat loss to the ambient from the free walls.

Also when the night times are observed, it is seen that as the height increase, temperature decrease. This is because, as the size of the vent gets bigger, the volume of the thermal wall decreases. This causes a decrease in the stored energy.

It can be concluded that the vent size must get smaller as it can. Though for this case it isn’t determined, if the vent size gets too small under a specific limit, it may not be as advantageous.

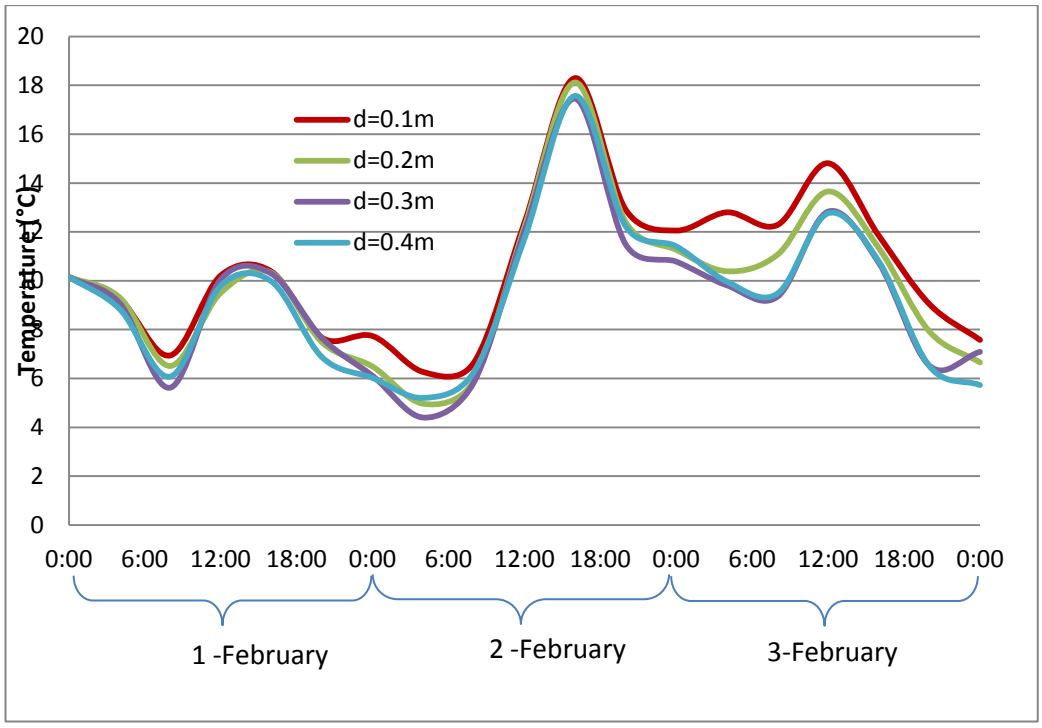

(a)

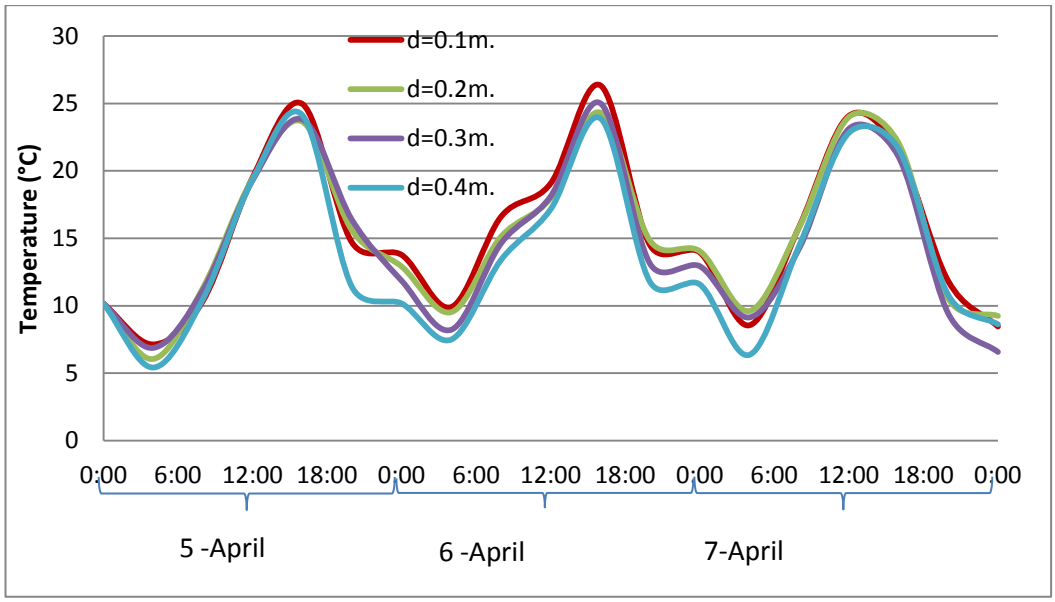

(b)

Figure 5.14: The 72 hour temperature variation of various vent heights*(d)* **(a)** winter conditions **(b)** spring conditions material comparison.

5.4.1.8. Thermal wall material variation results

The material of the thermal wall also affects the heating and cooling effect. This is because of the storage capacity of the thermal wall. The specific heating capacity, C_p of the material is a direct measure of the stored energy in it. Also, k, the thermal

conductivity is the measure that for how much heat is transmitted through the wall. The remaining energy will increase the temperature of the Trombe space air.

These simulations are made for the real case which is d=0.2m and t=0.2m. The thickness of the Trombe wall is the same for all material configurations which is 0.15 m. This means volume is kept constant. The C_p values are joules per mass Kelvin. For a case as this specific heat times density ($\rho_{mat} C_p$) should give a storage capacity per m^3 volume.

Table 5.4 : Used materials and properties.

Material	**Thermal Conductivity, k_{th} (W/mK)**	**Specific Heat Capacity, C_p (J/KgK)**	**Density, ρ (kg/m^3)**	**$\rho_{mat} C_p$ (J/m^3K)**
Concrete	1.4	880	2300	2024000
Wood	60.5	434	510	221340
Aluminum	237	903	2702	2439906

As seen from Table 5.4. If it is aimed to increase the heat storage capacity of the thermal wall, using metallic structures would give the best result. Not only the storage capacity per volume is higher, also the thermal conductivity is higher. This means, it will also transmit heat to the space more efficiently. The simulations are made with these three materials.

Figure 5.14 shows the results for winter and spring conditions. The graphs on Figure 5.15 show a significant difference between wood and the other two materials both in day and night time. The wood as the thermal storage ability is less than the other two causes a rapid increase in the air temperature. This is because the heat amount transmitted by the air is higher than the other two. But ability of usage as a heat storage, that is determined by the night temperature is very low with wood. The night temperatures drop rapidly, as the stored heat is low. The results for the concrete and aluminum material are very close to each other. That is actually surprising because aluminum is used as the best material for the thermal storage as mentioned in the literature review chapter.

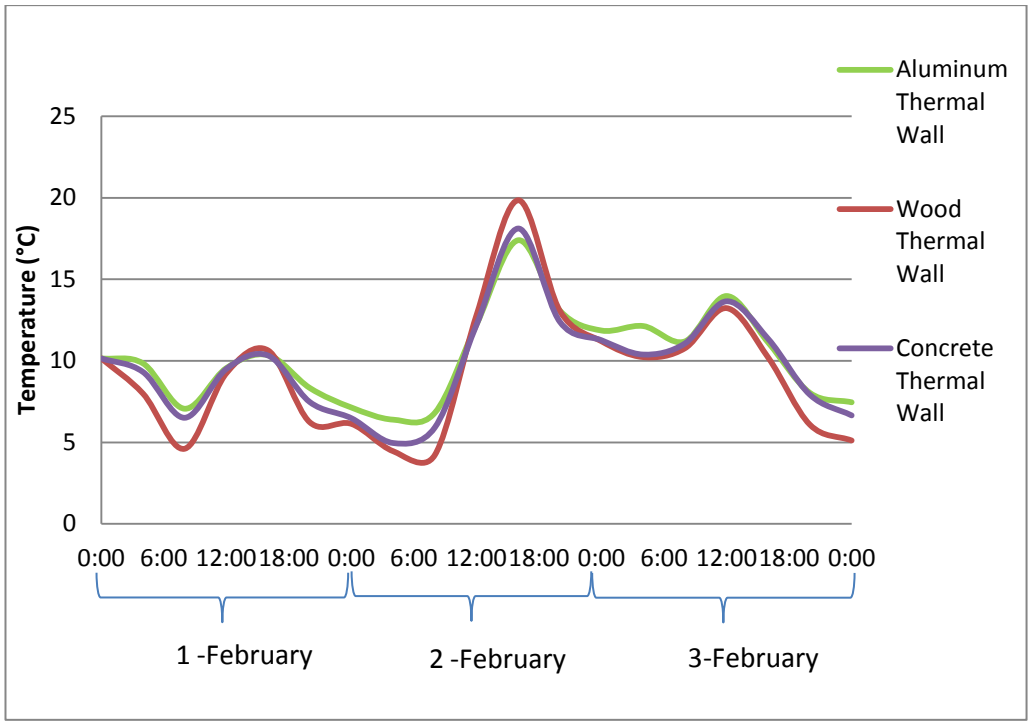

(a)

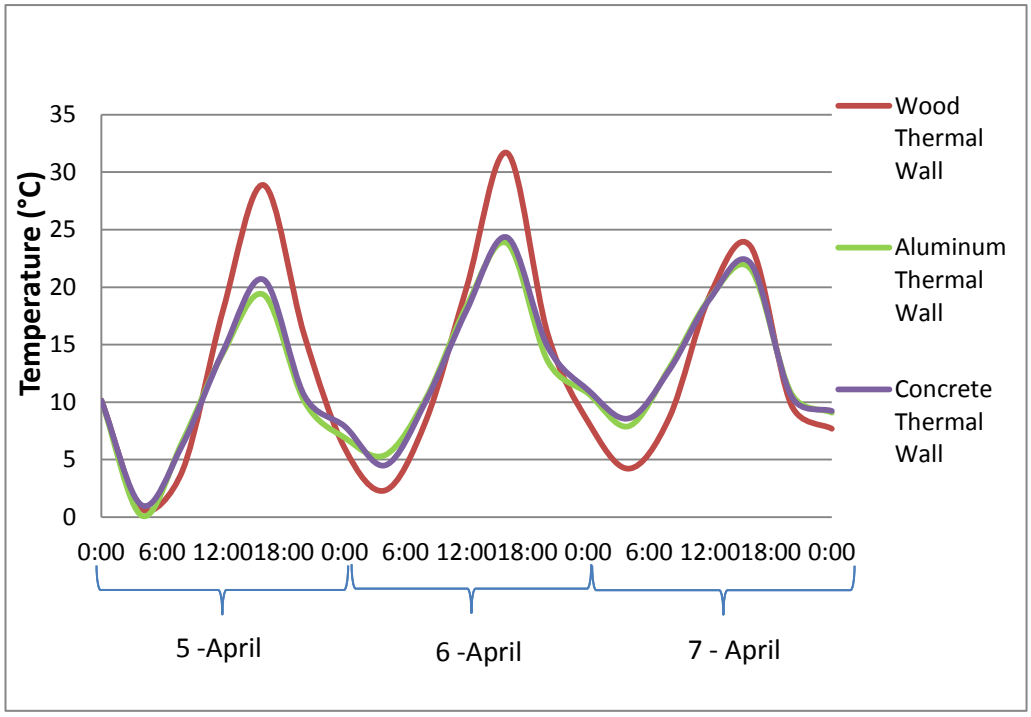

(b)

Figure 5.15: The 72 Hour Temperature Variation of Various Thermal Wall Materials **(a)** Winter Conditions **(b)** Spring Conditions Material Comparison.

Only a small amount of advantage is seen on night times. The advantage must be balanced with cost in order for application. For some cases, wood even can be beneficial. For a building occupied only at day times, such as an office complex, using wood thermal wall would increase the benefit from the sun.

5.4.2 3D simulation

2D analysis is used for time dependent simulation of the temperature behavior of the solar wall. Though, it is not possible to see the air flow in the domain realistically. Previously mentioned reductions prevent seeing the 3D flow in the domain.

To visualize the flow conditions in a better way, a 3D analysis has been run. 3D solution is not practical for a time dependent solution, since the element number of mesh will increase to hundred thousand. So, a steady – state analysis has been run for 3D analysis.

The boundary condition types are the same with the 2D analysis, only difference is that east and west walls are also introduced in the domain. So the heat transfer from these walls will also be considered.

5.4.2.1 Mesh

This time the 3D model of the geometry has been used. The same mesh dependence trial has been run for this configuration also. It turns out that the converged solution is mesh independent after a total of approximately 200000 elements.

The used mesh has about 380000 elements.

The wall boundaries have finer mesh in order to catch the wall boundary gradients.

The final mesh is seen on figure 5.16.

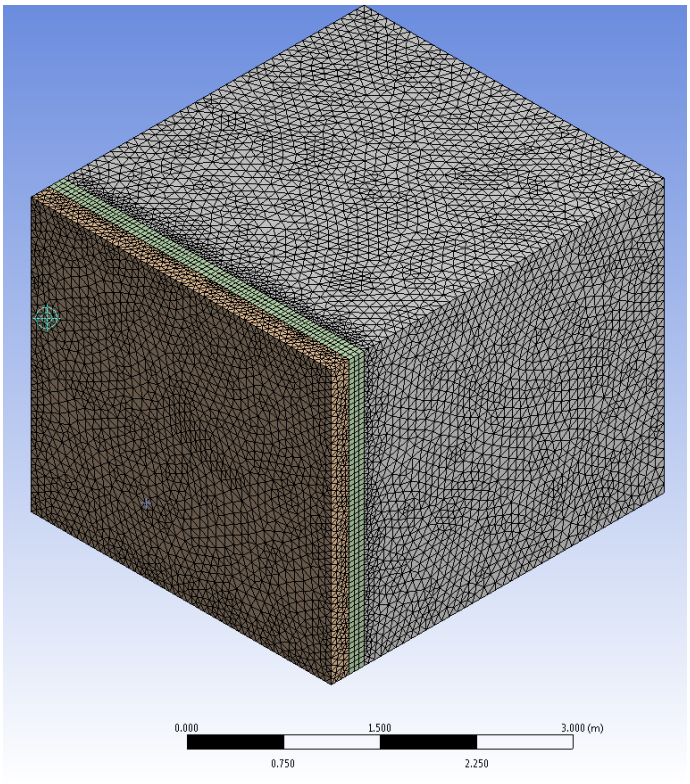

(a)

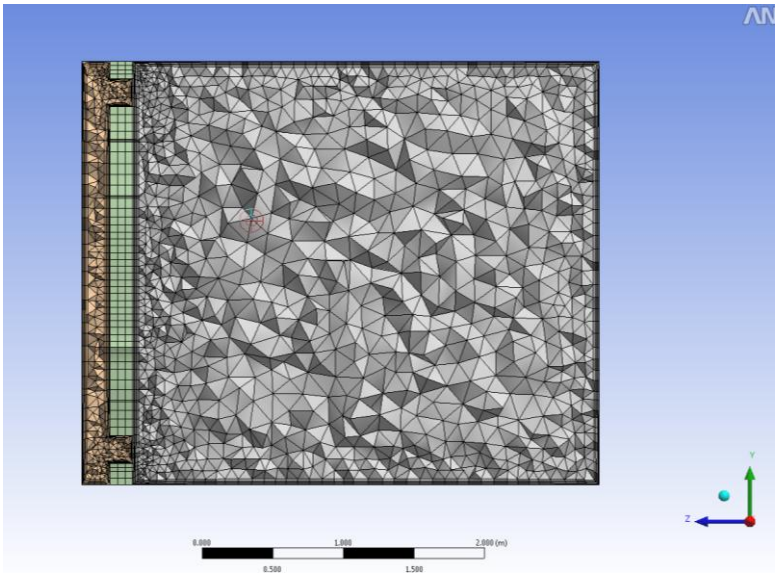

(b)

Figure 5.16 : 3D Grid **(a)** isometric view **(b)** side view inside cross section.

5.4.2.2 Boundary conditions

This time, different from the 2D time dependent analysis, all the boundary conditions are constant. Also this time, West and East walls are also boundaries. Table 5.5 shows these boundaries and related values.

Table 5.5 : Boundary conditions for 3D analysis.

Buoundary	**Boundary Condition Type**	**Value**	
Zone1Wall1 (Glazing)	Time Dependent Heat Flux	*Adiabatic*	
Zone1Wall3 (Solar Wall)	Time Dependent Heat Flux	*300 W/m^2*	
Floor	Constant Temperature	*9 °C*	
Roof	Wall Heat Transfer Coefficient and Outside Temperature	**Wall Heat Transfer Coefficient**	**Outside Temperature**
		20 W/m^2.K	*9 °C*
Zone2Wall3 (North Wall)	Wall Heat Transfer Coefficient and Outside Temperature	**Wall Heat Transfer Coefficient**	**Outside Temperature**
		20 W/m^2.K	*9 °C*
East and West Walls (Zone2Wall2 and Zone2Wall4)	Wall Heat Transfer Coefficient and Outside Temperature	**Wall Heat Transfer Coefficient**	**Outside Temperature**
		20 W/m^2.K	*9 °C*

The boundary conditions are chosen such that the flow inside the space will be able to visualize the flow conditions. Constant heat flux of *300 W/m^2* is estimated as a heating condition for the solar heat gains. This heat gain is given into domain from the sun exposed surface of the thermal wall. The configuration is for the outside temperature is 9 °C for all the walls. The real data is not considered this time but

imaginary boundary conditions are given for the simulation. The general behavior of the flow will be very similar to the real flow conditions in the building. The simulation is run for the real geometry which, trombe space thickness, t, is 0.2 and vent height, d, 0.2.

The simulation is again run with k-ϵ Turbulence model and Boussinnesq model is used for buoyancy effects.

5.4.2.3 3D Simulation results

These first results are for the Concrete thermal wall configuration. The velocity vectors and velocity contours in Figure 5.17 and Figure 5.18 show the flowing from the Trombe space to the main space very clearly. As seen the maximum velocities are seen close to the roof and floor. This flow should also cause a temperature difference between zones. Figure 5.19 shows this. The highest velocity is about 0.45 m/s. The air velocity in the zone where it is thought that will be occupied (the mid region of the domain) is not exceeding 0.25 m/s.

According to ASHRAE [33] Standard 55, this is between the comfort ranges. This standard states air speed below 0.2 m/s is the best for human comfort. The velocities between 0.2-0.4 m/s are perceivable but still in the comfort zone.

As seen from the temperature contours on Figure 5.19, the temperature is lower on than floor than the ceiling. Also it is observable to see the high temperatures near the wall.

Figure 5.20 shows the velocity contours inside the Trombe space. For the circulating air to heat more, this velocity is important. As mentioned before, also turbulence increases the heat transfer.

Figure 5.21 shows the turbulence kinetic energy contours. As seen, inside the Trombe space, turbulence kinetic energy, *k*, is relatively lower than the main space. Note that the higher k values are read where relatively fast flows develop. As mentioned earlier, k, affects the heat transfer coefficient. If day heating of air is demanded than turbulence inducer designs inside the Trombe wall could be made. Also, the turbulence is not demanded inside the main space. As heat transfer coefficient increases with turbulence, heat loss to the ambient from the walls also increase. The turbulence values can be reduced with designs.

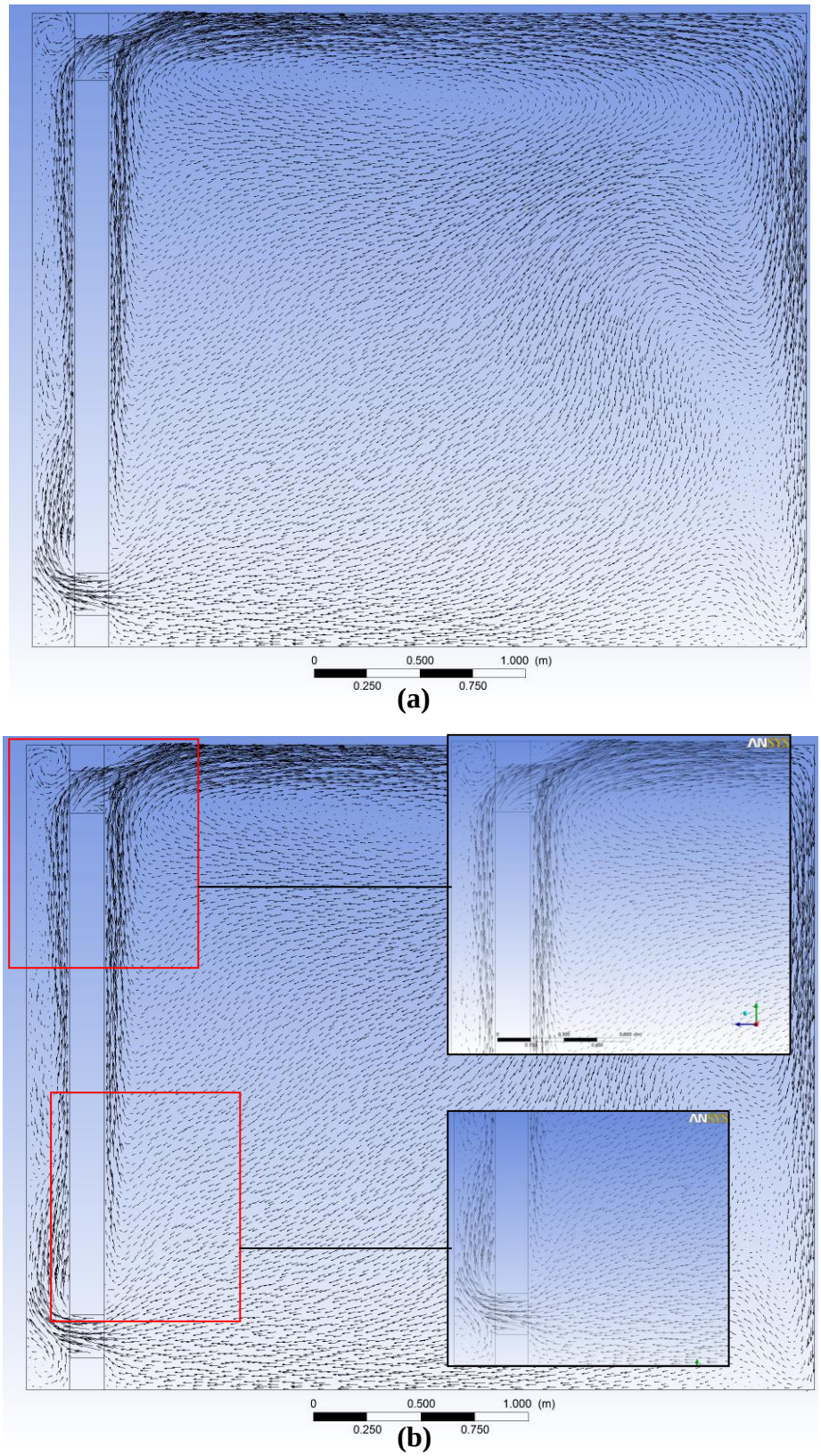

Figure 5.17 : The velocity vectors **(a)** for whole domain **(b)** for top and bottom vents.

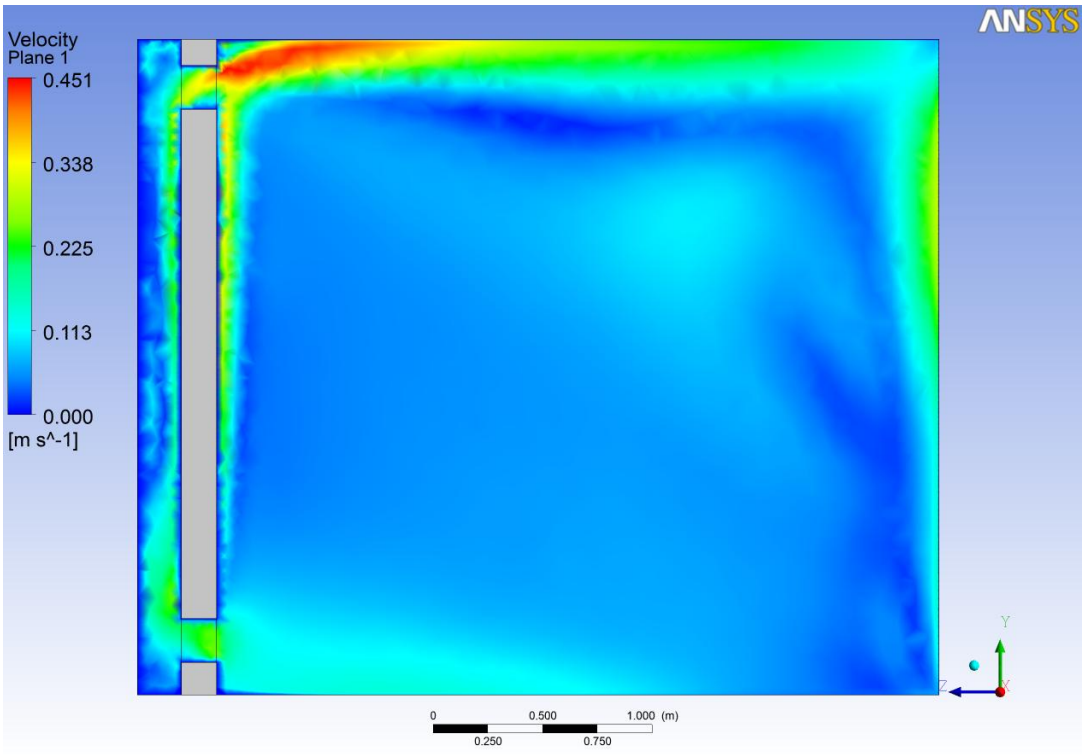

Figure 5.18 : Velocity contours of system.

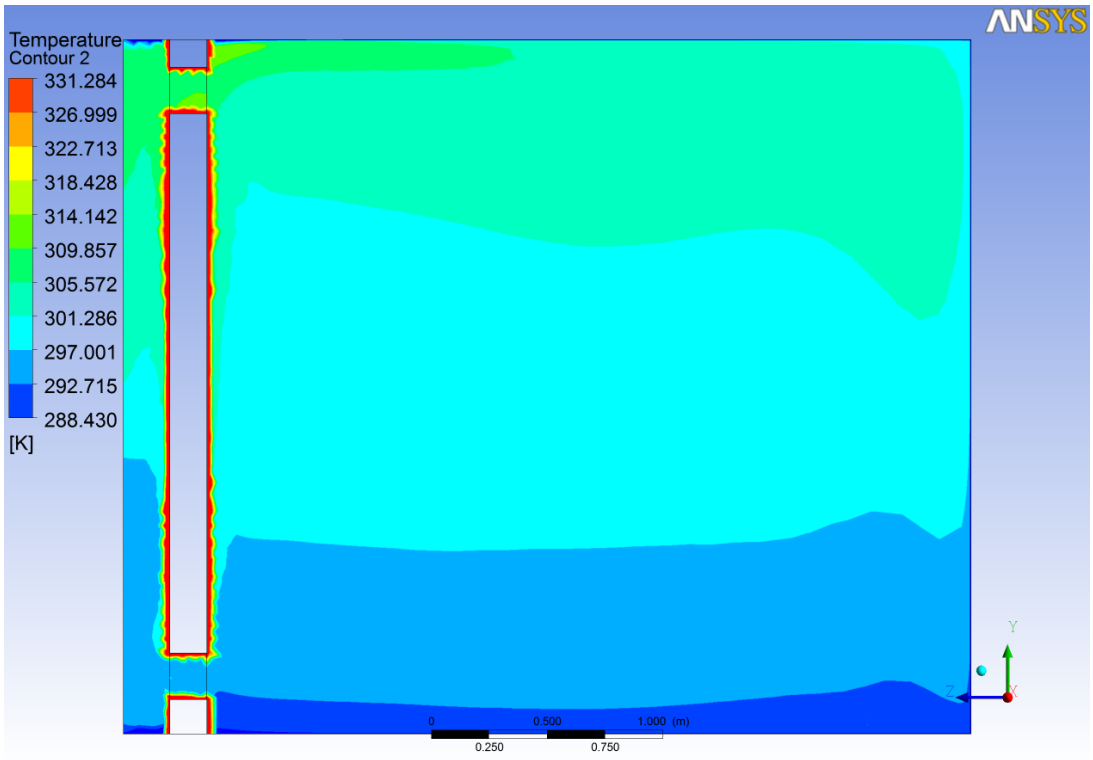

Figure 5.19 : Temperature contours in the space.

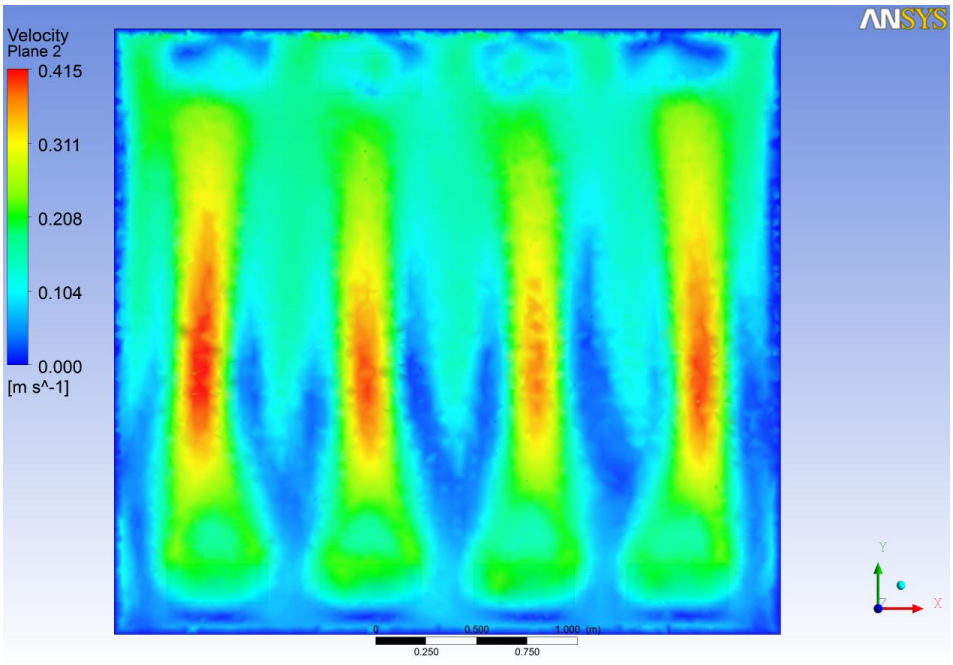

Figure 5.20 : Velocity contours inside the trombe space front view.

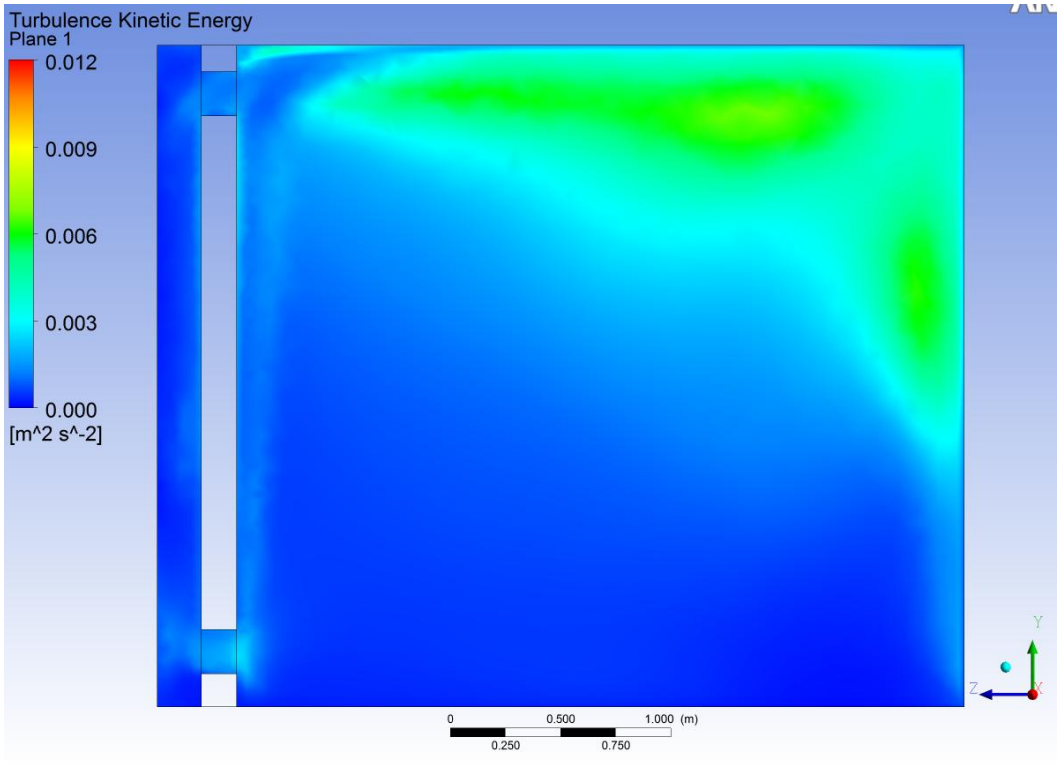

Figure 5.21: Turbulence kinetic energy contours of side view cross section.

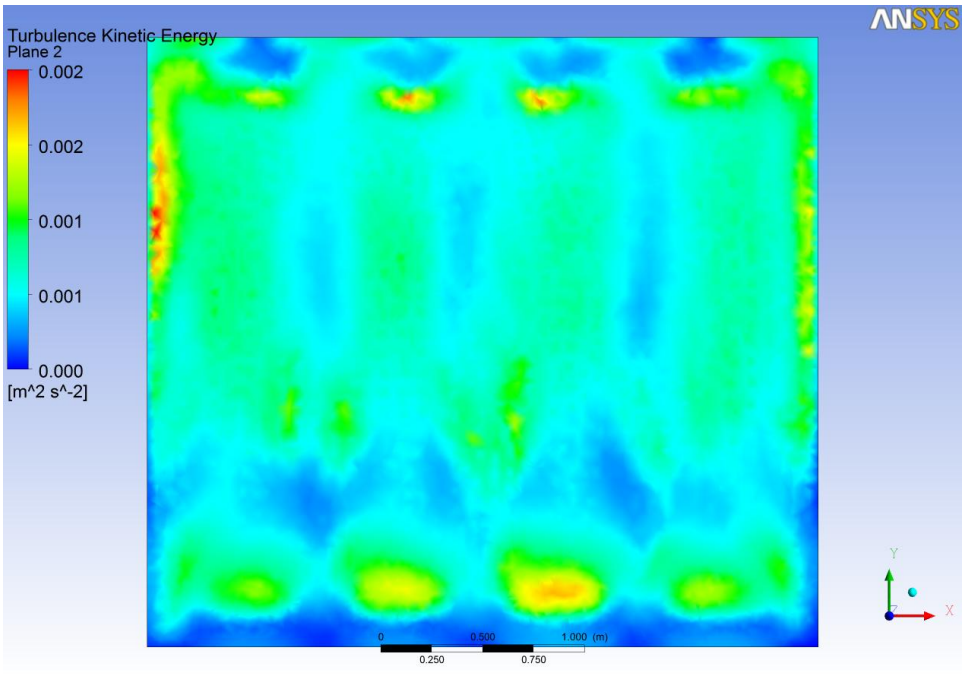

Figure 5.22 : Turbulence kinetic energy contours of front view cross section of trombe space.

6. CONCLUSION

This study presents a collection of analysis methods that can be used in optimizing a solar house using a Trombe wall.

The solar house concept is being widely used as the human being is trying to decrease the energy demand. Usage of fossil fuels is trying to be kept at minimum as possible. The renewable energy such as sun and wind usage plays an essential role for developing at this stage. Passive houses with zero energy usage is a very future promising study topic for the future as the only usage of the sun is not electricity generation but it can also be used for direct heating of spaces. As the buildings use about 25% of the generated energy and most of this energy is used by ventilation and heating systems, using renewable like sun for decreasing this demand is ingenious.

In this study, a very widely used system, solar walls, widely used passive house parts, are assessed. Though commercial usage of thermal walls can be seen, the optimization techniques are not very widely spread.

For optimization, building energy simulation (BES) and computational fluid dynamics (CFD) tools are both used. In contrast with the belief that CFD is a computationally expensive tool, with 2D reductions, practical analysis can be made.

Though BES is insufficient for complex flows, it can be very effective in solar radiation calculations. Coupling it with CFD, thermal walls can be optimized according to the conditions and occupations usages.

The results found in this study show that, some parameters affect the performance of the solar walls. Additional heat gain is expected from a solar wall. The question is when and how much to get it. It is shown that, with the same heat gain, it is possible to change the storage and day heating performances.

As an example, if the passive building is only occupied on daytimes, configuration parameters can be optimized to minimize the heat storage for the night and maximizing the daytime heating by finding the right parameters. Similarly, residences that are occupied on night mostly can be optimized to increase the heat storage and keep the space warm at nights.

Several variations can be made in order to optimize the solar walls. The design used in this study is relatively simple. Optimizing turbulence points, optimizing solar heat gain orientations, even calculating variable solar wall parameters such as controlled vents all can be analyzed with the technique used in this study.

The future study after this one can be to make this CFD – BES usage more practical and for the general user. Also studying the dynamic coupling of CFD and BES for vented thermal walls would be a stud that could be commercialized.

As the optimization and design techniques of the thermal walls spread, they will be very widely used in the close future.

REFERENCES

[1] Eurostat –Europian Comission, 2009, Panorama of energy, Energy statistics to support EU policies and solutions,

[2] SolarGIS © 2013 GeoModel Solar s.r.o., Solar Radiation Maps, Public Data

[3] Turkish State Meteorological Service Web Site < http://www.meteor.gov.tr > Viewed: 20.05.2013

[4] Passive House Alliance Web Site < http://www.phallience.com > Viewed: 20.05.2013

[5] Chel A., Nayak J.K., and Kaushik G., 2008, Energy conservation in honey storage building using Trombe wall, Energy and Buildings 40 p.1643–1650

[6] Wilson, A., Thermal storage wall Design manual, ©1979 NEW MEXICO SOLAR ENERGY ASSOCIATION

[7] Ellis, Peter G. 2003., Development and Validation of the Unvented Trombe Wall Model in EnergyPlus, Master's Thesis, University of Illinois at Urbana-Champaign

[8] Gan, G., 1998. A parametric study of Trombe walls for passive cooling of buildings. Energy Build. 27, Pages 37–43.

[9] Ghrab-Morcos, N., Bouden, C., Franchisseur, R., 1993. Overheatingcaused by passive solar elements in Tunis. Effectiveness of some way to prevent it. Renew. Energy 3 (6/7), Pages, 801–811.

[10] Hirunlabh, J., Kongduang, W., Namprakai, P., Khedari, J., 1999. Study of natural ventilation of houses by a metallic solar wall under tropical climate. Renew. Energy 18, Pages, 109–119.

[11] Stazi, F., Mastrucci, A., Perna, C.D., 2012, Trombe wall management in summer conditions:An experimental study, Solar Energy 86, Pages, 2839–2851

[12] Lai, C.M., Lin Y., 2011, Energy Saving Evaluation of the Ventilated BIPV Walls, Energies 2011, 4, Pages 948-959

[13] Url <http://www.solarwall.com>, Viewed: 23.04.2013

[14] Koyunbaba B.K., Yilmaz Z., Ulgena K., 2011, Energy and Buildings, Available online 28 June 2011

[15] Liu Y., Wang D., Ma .C., Liu J., 2013, A numerical and experimental analysis of the air vent management and heat storage characteristics of a trombe wall, Solar Energy, Volume 91, May 2013, Pages 1-10,

[16] Saadatian O., K. Sopian, C.H. Lim, Asim N., M.Y. Sulaiman, 2012, Trombe walls: A review of opportunities and challenges in research and development, Renewable and Sustainable Energy Reviews, Volume 16, Issue 8, October 2012, Pages 6340-6351

[17] Duffie, J. A. and W.A. Beckman, 2006. Solar Engineering of Thermal Processes. 3 Edition, John Wiley and Sons Inc.

[18] Internatianol Standard UNE-EN ISO 13790, 2004, Thermal performance of buildings—calculation of energy use for space heating.

[19] Ruiz-Pardo A., Domínguez S.A., Fernández J.A.S., 2010, Revision of the Trombe wall calculation method proposed by UNE-EN ISO 13790, Energy and Buildings, Volume 42, Issue 6, June 2010, Pages 763-773

[20] Shen J., Lassue S., Zalewski L., Huang D., 2007, Numerical study on thermal behavior of classical or composite Trombe solar walls, Energy and Buildings, Volume 39, Issue 8, August 2007, Pages 962-974

[21] K. Hami, B. Draoui, O. Hami, 2012, The thermal performances of a solar wall, Energy, Volume 39, Issue 1, March 2012, Pages 11-16,

[22] S. Jaber, S. Ajib, 2011, Optimum design of Trombe wall system in mediterranean region, Solar Energy, Volume 85, Issue 9, September 2011, Pages 1891-1898,

[23] Huseyin Onbasioglu, A.Nilufer Egrican, 2002, Experimental approach to the thermal response of passive systems, Energy Conversion and Management, Volume 43, Issue 15, October 2002, Pages 2053-2065

[24] Uygur S., Eğrican N., 1996, Modeling of natural turbulent flow in a passively heated zone, Energy Conversion and Management, Volume 37, Issue 5, May 1996, Pages 505-520,

[25] Hamza N., Underwood C., 2005, Cfd supported modelling of double skin facades in hot arid climates, Ninth International IBPSA Conference, Conference Paper.

[26] A. Mezrhab, M. Rabhi, 2008, Modeling of the thermal transfers in an enclosure of the trombe wall type, Thermodynamic Analysis in Renewable Energy, Jan 2008

[27] EnergyPlus, Engineering Reference

[28] Perez R.R, Ineichen P., Maxwell E.L., Seals R.D., Zelenka A., 1992, Dynamic Global to Direct Irradiance Conversiin Models, ASHRAE Transactions 1992

[29] ASHRAE Handbook, 2007

[30] Abraham J. P., Sparrow E. M., Minkowycz W. J., Internal-Flow Nusselt Numbers for the Low-Reynolds-Number End of the Laminar-to-Turbulent Transition Regime**,** Minnesota Supercomputing Instititu, Study Report.

[31] Ansys CFX , User's Guide 2011

[32] ANSI/ASHRAE Standard 62.2-2004, Ventilation and Acceptable Indoor Air Quality in Low-Rise Residential Buildings

[33] ANSI/ASHRAE Standard 55-1992, Thermal Environment Conditions for Human Occupancy

RESUME

He was born in 1986 in Ankara. He has finished Ankara Atatürk Anadolu Lisesi in 2004. He has graduated from Middle East Technical University Mechanical Engineering Department in 2009.